HHS Public Access

Author manuscript

*Brain Behav Evol*. Author manuscript; available in PMC 2016 May 27.

Published in final edited form as:

*Brain Behav Evol*. 2015 ; 85(3): 170–188. doi:10.1159/000381415.

# Elaboration and Innervation of the Vibrissal System in the Rock Hyrax (*Procavia capensis*)

**Diana K. Sarko**[1,*], **Frank L. Rice**[2], and **Roger L. Reep**[3]

[1] Dept of Anatomy, Cell Biology & Physiology, Edward Via College of Osteopathic Medicine, 350 Howard Street, Spartanburg, SC 29303

[2] Integrated Tissue Dynamics, 7 University Place, Suite B236, Rensselaer, NY 12144

[3] Department of Physiological Sciences, University of Florida, Gainesville, FL 32610

## Abstract

Mammalian tactile hairs are commonly found on specific, restricted regions of the body, but Florida manatees represent a unique exception, exhibiting follicle-sinus complexes (FSCs, also known as vibrissae or tactile hairs) on their entire body. The orders Sirenia (including manatees and dugongs) and Hyracoidea (hyraxes) are thought to have diverged approximately 60 mya, yet hyraxes are among the closest relatives to sirenians. We investigated the possibility that hyraxes, like manatees, are tactile specialists with vibrissae that cover the entire post-facial body. Previous studies suggested that rock hyraxes possess post-facial vibrissae in addition to pelage hair, but this observation was not verified through histological examination. Using a detailed immunohistochemical analysis, we characterized the gross morphology, innervation, and mechanoreceptors present in FSCs sampled from facial and post-facial vibrissae body regions to determine that the long post-facial hairs on the hyrax body are in fact true vibrissae. The types and relative densities of mechanoreceptors associated with each FSC also appeared to be relatively consistent between facial and post-facial FSCs. The presence of vibrissae covering the hyrax body presumably facilitates navigation in the dark caves and rocky crevices of the hyrax's environment where visual cues are limited, and may alert the animal to predatory or conspecific threats approaching the body. Furthermore, the presence of vibrissae on the post-facial body in both manatees and hyraxes indicates that this distribution may represent the ancestral condition for the supraorder Paenungulata.

### Keywords

vibrissae; FSC; somatosensory; Merkel endings; evolution; immunohistochemistry

## Introduction

Together with Proboscidae (elephants) and Sirenia (manatees and dugongs), the Hyracoidae (hyraxes) form the supraorder Paenungulata, or “nearly ungulates” [Ozawa et al. 1997; Simpson 1945]. Extant hyraxes comprise four species in three genera within the Family

[*]Corresponding author: D.K. Sarko, address as above, telephone: (864) 327-9847, fax: (864) 804-6986, dianasarko@gmail.com.

Procaviidae, two tree hyraxes (southern tree hyrax, *Dendrohyrax arboreus*; western tree hyrax, *Dendrohyrax dorsalis*) and two rock hyraxes (rock hyrax, *Procavia capensis*; yellow-spotted rock hyrax, *Heterohyrax brucei*) [Shoshani 2005]. Rock hyraxes are diurnal, rabbit-sized herbivores that inhabit rocky outcrops and mountainous regions predominantly in sub-Saharan Africa [Crandall 1964; Olds and Shoshani 1982; Stoddart and Fairall 1981; Walker et al. 1964]. They have a lifespan of approximately 12 years; subsist mainly on grasses, a low-quality and often scarce food source [Hoeck 1975; Olds and Shoshani 1982]; and also exhibit poor thermoregulation, forcing them to huddle together in low temperatures in order to conserve body heat [Sale 1970b] and to restrict feeding activities to cooler periods of each day [Brown and Downs 2006; Hoeck 1975]. Hyraxes generally live in family groups of one adult territorial male, several adult females, and their young [Hoeck 1975] and though they feed and sunbask as a group there is a high level of intraspecific aggression [Fourie 1977].

The orders Hyracoidea and Sirenia are thought to have diverged nearly 60 million years ago [Pardini et al. 2007; Springer et al. 2003], although the phylogeny of Afrotheria remains intensely debated based on analyses that focus on morphological or molecular traits, or both (e.g., [Asher et al. 2003; Cooper et al. 2014; de Jong 1998; Gheerbrant 2009; Kellogg et al. 2007; Kemp 2005; Kleinschmidt et al. 1986; Lavergne et al. 1996; Liu et al. 2001; Murata et al. 2003; Nishihara et al. 2009; Ozawa et al. 1997; Ruiz-Herrera and Robinson 2007; Shoshani and McKenna 1998; Springer et al. 1997; Springer et al. 2004]). Hyraxes appear to share many physiological characteristics with extant sirenia, including a low-quality food source and herbivorous lifestyle, poor thermoregulation, a relatively long gestation period, and few offspring [Olds and Shoshani 1982; Rubsamen et al. 1982; Sale 1970b]. The hyrax is also thought to share a sensory specialization otherwise present only in sirenians: a distribution of vibrissae (also known as tactile hairs or follicle-sinus complexes, FSCs) covering the entire body [Sale 1970a]. These appear as single, long black hairs interspersed among the shorter pelage fur (fig. 1a). Whereas the hyrax has an ample distribution of pelage hair in addition to presumptive vibrissae, vibrissae represent the only hair type found in Sirenia [Reep et al. 2002], based on the criteria of the follicle and its affiliated dense innervation being surrounded by a blood sinus encased within a thick connective tissue capsule [Rice et al. 1986].

Mammalian vibrissae are generally restricted to specific regions of the body, most notably the face (e.g., the mystacial vibrissae of rodents). In contrast, the expanded vibrissal system in the hyrax would presumably greatly increase spatial resolution and allow navigation in the rocky crevices of the hyrax habitat where poor illumination might impair visual discrimination. Indeed, hyraxes often enter small caves by reversing into them and have poor visual acuity for near objects [Sale 1970a]. Sale also noted that the hyrax's presumptive vibrissae have a wide distribution with optimal positioning for displacement by external sources of the animal's environment, including placement on the body regions of the anterior shoulder, carpal, back, flank, and caudal regions [Sale 1970a]. In dark, confined spaces, these hairs are stiffly erected, presumably to maximize contact with the surroundings [Sale 1970a] and thus they appear to have a sensory function [Hvass 1961]. Despite Sale's account of the presence of presumptive vibrissae, no histological verification exists. Further accounts of hyraxes possessing presumptive vibrissae are provided by Sokolov and Sale [Sokolov

1982; Sokolov and Sale 1981a, b] but also lack conclusive histological or immunohistochemical evidence classifying body hairs as vibrissae. Visual assessment confirms that single, long black hairs are interspersed among pelage fur in all four extant species of hyraxes.

Through systematic immunohistochemical analysis using anti-protein gene product 9.5 (PGP, a universal neuronal marker and cytoplasmic enzyme) as a standard in combination with antibodies against several other neural antigens, we were able to functionally characterize the innervation of hyrax vibrissal FSCs and to definitively determine for the first time that the long postfacial hairs on the hyrax body (fig. 1a) are in fact true vibrissae. Although the basic anatomical structure of FSCs remains relatively consistent across species, innervation patterns vary considerably under different evolutionary pressures and behavioral demands (e.g., [Ebara et al. 2002]). Therefore, through the investigation of an evolutionary outlier, examination of the expanded vibrissal system in hyraxes also represents a critical contribution to the understanding of mammalian sensory systems overall.

## Materials and Methods

Four adult hyraxes (*Procavia capensis*; 2 males and 2 females with weights ranging from 1.43-2.52 kg) were acquired from a licensed commercial supplier under IACUC protocol #E252. Animals were fasted for 24 hours prior to anesthesia. Anesthesia was induced briefly with 5% isoflurane in an induction chamber. The animal was then masked with 2% isoflurane and perfused through the left ventricle using phosphate-buffered heparinized saline (pH 7.0-7.4) at 37°C followed by 4% phosphate-buffered paraformaldehyde. Hair follicle samples were acquired from 9 body regions (fig. 1b): mystacial, submental, shoulder, and carpal; dorsal, lateral, and ventral aspects of the mid-region; and both caudal and tarsal regions (nomenclature follows [Sokolov and Kulikov 1987]). Follicle-sinus complexes were sampled as previously described [Reep et al. 1998] using a #11 scalpel blade to extract a block of tissue (approximately 5x5x15 mm) surrounding the follicle of interest. Follicles were cut mediolongitudinally to facilitate fixation immediately following dissection and placed in 4% paraformaldehyde overnight. After 24 hours of fixation follicles were removed and placed in 0.1M phosphate buffered saline (PBS; pH 7.0-7.4) and 30% sucrose. Sections were cut using a cryostat. Sections for conventional epifluorescence evaluation were cut at 14 μm parallel to the long axis of the follicles or in cross-section (perpendicular to the long axis of the follicles), then directly thawed onto slides subbed with chrome-alum gelatin. They were allowed to air dry, then immunolabeled on the slides. Follicles for confocal analysis were cut at 80 μm and free-floating sections were immunolabeled before being mounted onto slides. After labeling, the slides were coverslipped using either 90% glycerin in PBS or Vectashield (Vector Laboratories).

The sections were processed for single and double immunolabeling with the following primary antibodies:

1. Anti-protein gene product 9.5 (PGP, rabbit polyclonal, 1:800; UltraClone, Isle of Wright, UK; catalog #RA95101). The antigen was human PGP 9.5 protein purified

from pathogen-free human brain. The antibody shows one band at 26-28 kD on Western blot (tested in rabbits; [Wilkinson et al. 1989]). Anti-PGP has been found to be a universal neuronal marker in other species including rats [Fundin et al. 1997a; Rice et al. 1997], raccoons [Rice and Rasmusson 2000], monkeys [Pare et al. 2001; Pare et al. 2002], naked mole-rats [Park et al. 2003], humans [Albrecht et al. 2006], and Florida manatees [Sarko et al. 2007]. Controls for the specificity of PGP labeling were provided in these species by the use of pre-adsorption controls and the demonstration that labeling was limited to neuronal innervation and glia. Staining in hyrax follicle sections produced a pattern of immunoreactivity that was identical to descriptions in the previous studies of other species listed above.

2. Anti-neurofilament 200 kD subunit (NF, rabbit polyclonal, 1:800; Chemicon International, Temecula, CA,; catalog #AB1982, lot #24080051). The antigen was a highly purified bovine neurofilament polypeptide. The antibody labels phosphorylated and non-phosphorylated 200 kD NF and shows a band at 200 kD and bands around 170-180 kD on Western blot (tested in rabbits; manufacturer's technical information). Immunolabeling for this protein has been localized to myelinated fibers, including Aβ and Aδ fibers, and Merkel endings in a variety of species including rats [Fundin et al. 1997a; Rice et al. 1997], raccoons [Rice and Rasmusson 2000], monkeys [Pare et al. 2001; Pare et al. 2002], naked mole-rats [Park et al. 2003], humans [Albrecht et al. 2006], and manatees [Sarko et al. 2007]. Controls for the specificity of NF labeling were provided in these species by the use of pre-adsorption controls and the demonstration that labeling was limited to neuronal innervation and myelinated fibers. Staining in hyrax follicle sections produced a pattern of immunoreactivity that was identical to descriptions in the previous studies of other species listed above.

3. Anti-calcitonin gene-related peptide (CGRP, guinea pig polyclonal, 1:400; Peninsula Laboratories, Inc., San Carlos, CA; catalog #T-5027, lot #061121). The antigen is human α-CGRP with the following sequence: H-Ala-Cys-Asp-Thr-Ala-Thr-Cys-Val-Thr-His-Arg-Leu-Ala-Gly-Leu-Leu-Ser-Arg-Ser-Gly-Gly-Val-Val-Lys-Asn-Asn-Phe-Val-Pro-Thr-Asn-Val-Gly-Ser-Lys-Al a-Phe-NH2. The antibody has 100% reactivity with human and rat α-CGRP, human CGRP (8-37); chicken CGRP, human β-CGRP. It has 0.04% cross reactivity with human amylin and 0% cross reactivity with rat amylin and with human and salmon calcitonin (ELISA; manufacturer's technical information). Although Western blot information was not available, this protein has been localized to Merkel cells, C-fiber innervation, and vascular innervation in rats [Fundin et al. 1997a; Rice et al. 1997; Rosenfeld et al. 1983] and staining specificity has also been previously characterized in raccoons [Rice and Rasmusson 2000], monkeys [Pare et al. 2001; Pare et al. 2002], naked mole-rats [Park et al. 2003], humans [Albrecht et al. 2006], and manatees [Sarko et al. 2007]. Controls for the specificity of CGRP labeling were provided in these species by the use of pre-adsorption controls and the demonstration that labeling was characteristic of Merkel cells, C-fiber innervation, and vascular innervation. Staining in hyrax follicle sections produced a pattern of immunoreactivity that was identical to descriptions in the previous studies of other species listed above.

4. Anti-S-100 (S100, rabbit polyclonal, used neat; Biogenesis Inc., Brentwood, NH, catalog #8200-0184, lot #A2255). The antigen was purified bovine S100 protein. Although Western blot information was not available, this protein has been localized to brain glial cells and ependymal cells, in addition to Schwann cells of the peripheral nervous system and the antibody has been found to have no cross-reactivity in rats (manufacturer's technical information; [Moore 1965, 1982; Stefansson et al. 1982]. Controls for the specificity of S100 labeling were provided in other species including rats [Fundin et al. 1997a; Rice et al. 1997] and monkeys [Pare et al. 2001; Pare et al. 2002] by the use of pre-adsorption controls and the demonstration that labeling was limited to glia. Staining in hyrax follicle sections produced a pattern of immunoreactivity that was identical to descriptions in the previous studies of other species listed above.

5. Anti-BNaC1α (BNaC; rabbit polyclonal; 1:500; gift from Dr. Jaime García-Añoveros). The antigen was N-terminus peptide MDLKESPSEGSLQPSSC (corresponding to residues 1-16 of mouse, rat, and human BNaC1α; [Garcia-Anoveros et al. 2001]) and shows a band at 58.5 kD on Western blot in rats and mice [Garcia-Anoveros et al. 2001]. This protein is associated with low-threshold mechanoreceptors [Garcia-Anoveros et al. 2001]. Controls for the specificity of BNaC labeling were provided in these species by the use of pre-adsorption controls and the demonstration that labeling was limited to low-threshold mechanoreceptors. Staining in hyrax follicle sections produced a pattern of immunoreactivity that appeared identical to descriptions in the previous studies of other species listed above. Hyrax follicle tissue was also prepared without each primary antibody as a control for the specificity of the secondary antiserum. Western blots could not be performed on hyrax tissue due to the low availability of fresh tissue samples.

6. Anti-neuropeptide Y (NPY; sheep polyclonal, 1:1,000; Chemicon International, Inc.; catalog # AB1583). Staining in hyrax follicle sections produced a pattern of immunoreactivity that appeared identical to descriptions in the previous studies of other species listed above. Although Western blot information was not available, manufacturer's information, controls for the specificity of labeling were provided by the use of pre-adsorption controls and the demonstration that labeling was limited to sympathetic innervation. Antibody specificity was determined by radioimmunoassay: synthetic peptides somatostatin-14, leu-enkephalin, met-enkephalin, oxytocin, Agr8-vasopressin, vasoactive intestinal peptide and angiotensin II showed less than 0.005% cross reactivity and substance P less than 0.02%; peptide YY and bovine pancreatic polypeptide showed approximately 36% and 0.05% cross reactivity respectively; human Peptide YY shares 65% homology amino acid sequence for human NPY (RIA; manufacturer's technical information).

Primary antibodies against myelin basic protein (MBP; mouse monoclonal, 1:1,000; Sternberger Monoclonals, Lutherville, MD, cat. no. SMI99, lot no. 1), tyrosine hydroxylase (TH; rabbit polyclonal, 1:800; Chemicon International, Inc.), and TrpV1/VR1 (vanilloid receptor 1; capsacin binder; guinea pig polyclonal, 1:1,000; Neuromics Antibodies, Northfield, MN, cat. no. GP14100, lot no. 400511) used successfully in previous rat,

monkey and human studies [Albrecht et al. 2006; Fundin et al. 1997a; Pare et al. 2001] did not produce significant labeling on hyrax tissue.

All thin (14 μm) sections were first preincubated with 1% bovine serum albumin (BSA) and 0.3% Triton X-100 in 0.1M PBS for 1 hour, then incubated with a solution of primary antibody (diluted in PBS with 4% calf serum or 1% BSA and 0.3% Triton X-100) overnight at 4°C at high humidity. Slides were then rinsed in PBS for 30 minutes and subsequently incubated in the dark at room temperature for 2 hours with Cy3- (for red fluorescence; 1:500) and Alexa488- or Cy2- (for green fluorescence; 1:250) conjugated secondary antibodies (Molecular Probes, Inc., Eugene, OR; Jackson Immunoresearch Laboratories, Inc., West Grove, PA) diluted in PBS or BSA with 0.3% Triton X-100. Slides were then rinsed in PBS and either temporarily coverslipped under PBS (in the case of future double labeling) or coverslipped with 90% glycerol in PBS. Double labeling was usually accomplished by repeating the immunofluorescence procedure described above. In some cases double labeling was achieved through a single cycle of incubations beginning with a 1:1 mix of the monoclonal and polyclonal primary antibodies. To control for non-specific labeling, incubation with primary antibody was omitted or the primary antibody was preincubated with a specific blocking peptide. The thick (80 μm) sections were processed free-floating in the same antibody dilutions as in the thinner sections. Incubations were for 2 days in primary antibodies and overnight in secondary antibodies at 4°C. Rinses were for at least 4 hours.

Sections were analyzed with an Olympus Provis AX70 microscope equipped with conventional fluorescence: 1) Cy3 filters (528-553 nm excitation, 590-650 nm emission), and 2) Cy2 filters (460-500 nm excitation, 510-560 nm emission). Fluorescence images were captured with a high resolution (1280 × 1024 pixels) three chip color CCD camera (Sony, DKC-ST5) interfaced with Northern Eclipse software (Empix Imaging, Inc., Mississauga, ON). Images were de-blurred using a deconvolution program based on a 1 μm, 2-dimensional nearest neighbor paradigm (Empix Imaging, Inc., Mississauga, ON). Samples were imaged on a Zeiss LSM 510Meta confocal microscope (Carl Zeiss MicoImaging, Inc., Thornwood, NY) equipped with an Argon (488 nm excitation) and a green HeNe (543 nm excitation) laser. Emissions were collected using a Band Pass 500-530 nm emission filter for Alexa Fluor 488. For Cy3 either a Long Pass 560 nm emission filter or a Band Pass 560-615 nm emission filter was used, depending on whether the sample was single or double labeled. Images were collected with a Plan-Neofluor 25x/0.8 Imm corr DIC lens with the pinhole set for 1 Airy Unit. Confocal image Z-stacks were collected at 512 x 512 pixel x-y resolution and 1μm steps in Z. Three-dimentional (3D) surface rendered images were produced using the VolumeJ plug-in for ImageJ software (http://rsb.info.nih.gov/ij/).

Since the intensity of immunolabeling for the numerous antibodies used in the present study is attributed to many variables that cannot be individually quantified, this study does not attempt to quantify the relative amounts of labeled antigens. These variables include: 1) true differences in the presence and quantity of the antigen, 2) whether the antibody is monoclonal or polyclonal, 3) background labeling, 4) antibody concentration, 5) antibody efficacy, and 6) location of the antigen (i.e., membrane or cytosol). Because the labeling intensities differed between the various types of antibodies, the photomicrographs compiled

for illustrative purposes were adjusted using Northern Eclipse, Adobe Photoshop (San Jose, CA) software so that the maximum labeling contrast and intensity were similar for each antibody.

## Results

The presumptive vibrissae appear as single, elongated black hairs interspersed among the pelage fur on all parts of the hyrax body (fig. 1a). The basic structure and overall innervation of the follicles for these elongated black hairs on all 9 body regions examined (fig. 1b), including the mystacial pads, revealed that these hairs are true vibrissae that emanate from follicle-sinus complexes (FSCs) as shown schematically in figure 2 and immunohistochemically in figure 3. The FSCs each consisted of a follicle core, affiliated dense innervation, and a surrounding blood sinus enclosed within a thick connective tissue capsule [Rice et al. 1986] along with a prominent ringwulst. Although the gross morphology of mystacial FSCs exhibited pronounced elongation compared to non-mystacial FSCs, similar innervation patterns were present in the FSCs across all body regions (fig. 2-3). The FSCs from all body regions were innervated by two deep vibrissal nerves that penetrated the thick FSC capsule bilaterally at the cavernous sinus level and supplied sensory endings primarily to the ring sinus level. Several superficial vibrissal nerves supplied innervation primarily to the rete ridge collar as well as the outer and inner conical body levels of each FSC in addition to innervating adjacent skin and guard hairs. As observed in manatees, no papillary muscle slings – which are present in most other species examined to date – were observed in association with any of the hyrax FSCs including those on the mystacial pad.

The dermis surrounding the capsule of each hyrax FSC contained numerous blood vessels that were densely innervated by a variety of thin-caliber fibers that either labeled with anti-NPY (and therefore constituted presumptive sympathetic innervation) or that expressed CGRP immunoreactivity (fig. 2; fig. 4a-b). The CGRP-positive vascular innervation included both NF-negative and NF- positive thin-caliber fibers that were presumptive C and Aδ fibers, respectively, and were presumably sensory. Peptidergic (CGRP-positive, NF-negative) and nonpeptidergic (CGRP-negative and NF-negative) C-fiber innervation was also associated with each FSC at the rete ridge collar level.

### Innervation to the mouth of the FSCs and surrounding epidermis

The hyrax skin and rete ridge collar (RRC, the invagination of the skin toward the FSC) exhibited moderate innervation penetrating the epidermis, including thin-caliber fibers, most of which were NF200-negative and some of which were either CGRP-positive or CGRP-negative (fig. 4c-e). The remaining fibers labeled for both anti-PGP and anti-NF200. It has been shown in other species that NF-negative fibers are characterized as thin-caliber, MBP (myelin basic protein)-negative fibers, indicating that they are C fibers. In contrast, NF-positive fibers can be thin or thick-caliber and consistently co-label for anti-MBP, indicating that they are Aδ or Aβ fibers, respectively [Albrecht et al. 2006; Fundin et al. 1997a; Pare et al. 2001; Rice and Rasmusson 2000]. Thus, the majority of the innervation to the rete ridge of the FSCs included presumptive free nerve endings (FNEs) associated with C fibers, in addition to a lesser degree of Aδ fiber innervation (fig. 5a). No Pacinian corpuscles or

Meissner corpuscles were observed. Numerous Merkel ending complexes (MECs) were observed terminating at the RRC of hyrax FSCs and at the base of the adjacent epidermis in all areas (fig. 3a, d; fig. 4c-e). These complexes consisted of Merkel endings, which colabeled with NF200 and PGP, and associated with Merkel cells, which colabeled with CGRP and PGP. An unusual feature of Merkel innervation in hyrax FSCs included semicircular dermal bulges laden with Merkel ending complexes at the RRC level (fig. 3a, d; fig. 4c-e; fig. 5c-d). These have not been seen in FSCs of any other species examined to date, but did resemble the Merkel innervated rete pegs in the glabrous skin of the raccoon [Rice and Rasmusson 2000].

Progressing deep to the rete ridge collar, the connective tissue capsule of each FSC had a relatively narrow site of convergence (known as the outer conical body, or OCB) at the "neck" of the FSC. Prominent circumferential sebaceous glands were evident at the outer conical body level (fig. 3a, d; fig. 6a) and were particularly evident in mystacial, submental, and carpal FSCs.

## Innervation to the inner conical body

The outer conical body of the hyrax FSC enclosed a less compact region of connective tissue (the inner conical body, or ICB; figs. 2-4). The ICB level of hyrax FSCs contained only a paucity of fine-caliber fibers that presumably terminated as free nerve endings (FNEs; fig. 5b; fig. 6b). The majority of these fine-caliber fibers labeled only with anti-PGP (presumptive sympathetic innervation) and a subset co-expressed CGRP or NF200 immunoreactivity (fig. 3b; fig. 7a-c). No transverse lanceolate endings, such as those seen in rodent FSCs, were observed at the inner conical body level of hyrax FSCs across all body regions sampled. There were also no trabeculae at the superficial end of the ring sinus, differing from the arrangement observed in manatees [Sarko et al. 2007].

## Innervation at the ring sinus level

Mystacial FSCs exhibited an unusual morphology with longitudinal ridges and grooves extending up from the cavernous sinus to the lower ring sinus level. These were particularly evident in cross sections through the FSC (fig. 6d-e). Not observed in any other species to date, these grooves were packed with axons ascending from the DVNs (fig. 6d-e).

Large-caliber Aβ fibers ascended from the deep vibrissal nerve in each hyrax FSC to supply dense networks of Merkel ending complexes. Merkel ending complexes appeared to be uniformly distributed in the outer root sheath surrounding each follicle (fig. 3; fig. 4c; fig. 5e; fig. 6c; fig. 7e), labeled positively for BNaC, and are known to be slowly adapting mechanoreceptors. Each Aβ fiber that terminated as Merkel endings branched extensively to form numerous endings that ramified over the circumference of the follicle (fig. 7b-c).

Each FSC had an unusually thick mesenchymal sheath (fig. 6b-c) coating the basement membrane of the follicle at the levels of the ring sinus and cavernous sinus. A limited distribution of longitudinal lanceolate endings were observed at the upper ring sinus level (fig. 7d). In addition, "tangle" endings, described previously only in Florida manatees [Sarko et al. 2007], were supplied by large-caliber DVN Aβ fibers and terminated within the mesenchymal sheath at the upper ring sinus/lower ICB level (fig. 7b, e). Though apparently

smaller compared to those observed in manatees, each tangle ending had characteristic “tangles” of NF-positive fibers within a PGP-positive cytoplasmic envelope and was associated with terminal glia.

At the level of the ringwulst, mesenchymal bulges caused innervation from the DVN to curve around the bulges as it ascended superficially through the ring sinus level (fig. 3a-b, d, arrowheads; fig. 7a-c, arrowheads). Club endings (unbranched terminations of Aβ fibers first described by [Ebara et al. 2002]) were widely and uniformly spaced around the perimeter of the mesenchymal sheath at the level where the prominent, well-defined ringwulst was attached (fig. 3a; fig. 5f; fig. 7a-b). The mesenchymal sheath also contained a sparse distribution of thin-caliber fibers lacking morphologically distinct endings, presumably forming FNEs.

### Innervation at the cavernous sinus level and hair papilla

No large caliber innervation was found within the trabeculated cavernous sinus (CS; fig. 3; fig. 4c; fig. 6d-e). Instead, innervation resided in closer proximity to the follicle along the mesenchymal sheath. As seen in other species, spiny endings were observed at the more superficial extent of the CS, near the ring sinus (fig. 3c, fig. 8a), but were sparsely distributed as terminations of Aβ fibers. Reticular-like endings were also observed at this level, were associated with Aβ fibers, and appeared to project into pockets or papillae (fig. 3b-c; fig. 8b). Finally, sparsely distributed spray endings of Aβ fibers were observed in the cavernous sinus (fig. 8b). Spray endings, along with spiny and reticular endings, colabeled for NF200 and PGP. The hair papilla exhibited only sparse, fine-caliber innervation that was not superficially extensive (fig. 8c). This innervation included Aδ (NF200+/PGP+) fibers as well as C fibers (CGRP+/NF200-/PGP+) terminating as presumptive free nerve endings (fig. 8d-e).

### Guard hairs

Although not the focus of the present study (and therefore not characterized in detail), guard hairs proximal to vibrissae were observed (fig. 9). These hairs lacked the circumferential, blood-filled ring sinus and dense connective tissue capsule that characterize FSCs. Guard hairs were associated with prominent sebaceous glands and piloneural complexes that included circumferential longitudinal lanceolate endings which labeled for NF200, PGP, and S100 (fig. 9).

## Discussion

### Innervation of follicle-sinus complexes

The present report is the first to confirm that the expanded, body-wide distribution of elongated hairs, interspersed among pelage hair on the rock hyrax body, are in fact true vibrissae, exhibiting the definitive traits of a circumferential blood sinus, a variety of innervated mechanoreceptors, and a dense connective tissue capsule [Rice et al. 1986]. Merkel ending complexes were the predominant form of mechanoreceptor type found in hyrax FSCs. These were affiliated with large-caliber Aβ fibers ascending from the deep vibrissal nerve to terminate predominantly in the outer root sheath at the ring sinus level.

Merkel ending complexes exhibited two unusual features in rock hyraxes: 1) semicircular bulges laden with Merkel ending complexes that appeared to surround dermal ridges at the RRC level, and 2) mesenchymal bulges at the level of the ringwulst that were affiliated with Merkel ending complexes as innervation from the deep vibrissal nerve ascended superficially through the ring sinus. Merkel endings are low threshold, slowly adapting mechanoreceptors integral in detecting compression as well as directionality of a stimulus during tactile discrimination [Gottschaldt and Vahle-Hinz 1981; Iggo 1963, 1966; Iggo and Muir 1969; Johansson and Vallbo 1983; Johansson et al. 1982a, b; Lichtenstein et al. 1990; Munger et al. 1971; Rice et al. 1986]. Merkel endings at the RRC are likely to detect large-angle hair deflections whereas endings at the ring sinus level presumably respond to more discrete perturbations, thus serving complementary roles based on where they are distributed within the FSC [Gottschaldt et al. 1973; Rice et al. 1986]. The dense distribution of Merkel ending complexes in FSCs across all body regions of the hyrax indicates a particular investment in directionality detection when a vibrissa is deflected [Burgess and Perl 1973; Rice et al. 1986]. Similarly, Merkel ending complexes were the predominant type of mechanoreceptor present in manatee FSCs, although likely facilitating detection of underwater stimuli in the manatee's case [Sarko et al. 2007] as opposed to detection of rocky crevice surroundings for the rock hyrax.

Club-like endings, present at the attachment site of the ringwulst, indicate sensitivity to mechanical perturbations at this location in hyrax FSCs. These mechanoreceptors were also present in manatees [Sarko et al. 2007] and likely respond to displacement of the ringwulst, situated within the blood-filled ring sinus, relative to the hair shaft of the follicle [Ebara et al. 2002]. In addition to club endings, a sparse distribution of longitudinal lanceolate endings was detected along the upper (more superficial) extent of the ring sinus. Lanceolate endings are low-threshold, rapidly adapting stretch receptors encoding aspects of vibrissal movement such as acceleration and deceleration of deflection [Burgess and Perl 1973; Gottschaldt et al. 1973; Lichtenstein et al. 1990; Rice et al. 1997; Rice et al. 1986; Tuckett 1978; Tuckett et al. 1978]. The low density of distribution for lanceolate endings and a high distribution of Merkel endings in both manatees [Sarko et al. 2007] and rock hyraxes emphasizes an investment in detecting the presence or absence of a stimulus - and the direction of origin for that stimulus - over dynamic stimulus properties such as speed of vibrissal deflection. Dense palisades of longitudinal lanceolate endings were however detected in pelage hair, indicating that these hairs are attuned to speed of displacement. Given these disparate mechanoreceptor distributions, vibrissae and pelage may serve complementary roles on the hyrax body. Presumably, initial detection of surrounding substrates (e.g., holes or rock crevices) or threats would first deflect elongated vibrissae that extend further from the body, signaling directionality of the contact. Subsequently, as the stimulus approaches more closely to the hyrax body, pelage hair deflection (in addition to large-angle deflection of vibrissae) might signal speed of contact.

“Tangle endings,” described previously only in Florida manatees [Sarko et al. 2007], were also present within rock hyrax FSCs; terminated in similar locations (along the mesenchymal sheath of the upper ring sinus/lower ICB level); and exhibited similar immunohistochemical characteristics as “tangles” of NF-positive fibers within a PGP-positive cytoplasmic envelope associated with glia. The rock hyrax tangle endings were

notably smaller compared to those observed in the manatee, possibly due to relative scaling with body size or diminished function. In manatees, tangle endings were present in both facial and postfacial FSCs and were thought to enhance directionality detection [Sarko et al. 2007].

A second type of novel mechanoreceptor previously described only in manatee facial vibrissae [Sarko et al. 2007], the trabecular ending, was not detected in rock hyrax FSCs. These mechanoreceptors were thought to be an adaptation to detection of underwater stimuli, particularly in detecting tension along the trabeculae as the particularly rigid manatee facial vibrissae are deflected [Sarko et al. 2007]. In fact, innervation was absent in the rock hyrax FSC cavernous sinus, and branches from the deep vibrissal nerve terminated exclusively along the mesenchymal sheath. The absence of trabecular endings in rock hyraxes supports the hypothesis that these mechanoreceptors are an aquatic adaptation optimized to facilitate tactile exploration and object recognition. Instead, spiny and reticular endings – absent in manatees, but present in rock hyrax FSCs – may serve a related function. These endings have been noted in a wide range of species in the cavernous sinus and are thought to detect stresses within the mesenchymal sheath parallel to the long axis of the follicle, in the case of spiny endings, or to detect tension perpendicular to the long axis of the follicle with directional sensitivity, in the case of reticular endings [Ebara et al. 2002; Fundin et al. 1997b; Rice et al. 1997].

### Vibrissae: comparative distribution

In most terrestrial mammals vibrissae are found only on restricted regions of the body, and are particularly concentrated on the face [Eisenberg 1981; Pocock 1914]. Some rodents possess a few carpal, antebrachial or tarsal vibrissae [Fundin et al. 1995], and a few vibrissae are found on the trunk in two squirrel species [Hyvärinen et al. 1977; Sokolov and Kulikov 1987]. Naked mole-rats exhibit an expanded system of body hairs that function as tactile hairs but are enlarged guard hairs lacking affiliated FSCs rather than true vibrissae [Crish et al. 2003]. In contrast, hyraxes exhibit an expanded, body-wide distribution of vibrissae interspersed among pelage fur.

Similar to terrestrial mammals, most marine mammals also exhibit a restricted distribution of vibrissae. Pinnipeds and cetaceans have vibrissae on the head only [Ling 1977]. Pinnipeds exhibit morphological elaborations of the vibrissae that are associated with prey capture and benthic foraging [Ginter et al. 2012; Marshall et al. 2006]. Baleen whales have approximately 100 thin vibrissae on the upper and lower jaws, and some exhibit tubercles on the head that contain innervated hairs [Mercado 2014]. In most odontocete cetaceans, hair is present only as prenatal vibrissae which atrophy, resulting in vibrissal crypts which are electroreceptive in some taxa [Czech-Damal et al. 2013; Czech-Damal et al. 2012; Ling 1977]. An important exception is freshwater river dolphins, which have well-developed vibrissae along the upper and lower jaws that may be used in prey localization [Layne and Caldwell 1964; Ling 1977]. As first described by Dosch in dugongs and later verified in manatees, sirenians are unusual in having vibrissae distributed over the entire body, and this is the only type of hair they possess [Bryden et al. 1978; Dosch 1915; Kamiya and Yamasaki 1981; Reep et al. 2002; Reep et al. 1998; Reep et al. 2001; Sokolov 1986]. Marine mammals

of the order Sirenia, among the hyrax's closest extant relatives, are the only other species known to exhibit this elaborated pattern of true vibrissae distributed on the entire body [Reep et al. 2002; Sarko et al. 2011]. This elaboration of vibrissal distribution appears to have been adaptive enough to be conserved across the Orders Sirenia and Hyracoidae.

## Vibrissae evolution and comparative function

Vibrissae facilitate a wide range of perceptual and behavioral functions, including spatial orientation and navigation in rodents (e.g., [Brecht et al. 1997; Sokolov and Kulikov 1987]); object discrimination and prey detection in Australian water rats [Dehnhardt et al. 1999]; social display in pinnipeds [Miller 1975]; tracking hydrodynamic trails in harbor seals [Dehnhardt et al. 2001]; and oripulation in manatees [Marshall et al. 1998; Reep et al. 2001]. Hyraxes are the only terrestrial mammals with a body-wide distribution of vibrissae, although some rodents have several postfacial vibrissae associated with restricted body regions and likely used for spatial orientation (e.g., in arboreal environments). The principal utility of vibrissae in the rock hyrax may center around predator avoidance. Because hyraxes are slow-moving and possess few defense mechanisms against predators (mainly leopards, snakes, caracals, wild dogs, and eagles [Coe 1962; Turner and Watson 1965]), they appear to depend on rock crevices for safety, escape, and survival [Fairall et al. 1983]. In addition, hyraxes will inhabit holes that they have dug for themselves in the ground [Shortridge 1934] or that have been usurped from aardvarks or meerkats [Roberts 1951]. These holes are often small – “no deeper than an adult hyrax in a crouching position” – with entrances too small to permit entrance to the larger and more frequent predators [Sale 1966]. Seasonal food availability – and a balance between foraging or grazing versus predation risk – may be an integral component as well. The low-quality and scarce food sources of the rock hyrax drive more frequent foraging at greater distances (>50 m) in the winter, increasing risk when the dense vegetative cover that is present in summer cannot be relied on in addition to close proximity to rock crevices [Brown and Downs 2006]. Holes and crevices appear to offer not only protection, but also water retention, proximity to vegetation, and climactic moderation that is somewhat sheltered from surrounding fluctuations [Turner and Watson 1965]. Presumably, a distribution of vibrissae on the hyrax body would enhance detection of those protective boundaries within holes and crevices, guiding navigation and enhancing survival where visual cues are minimal. In Hebrew, rock hyraxes are known as “Shaphan,” translating as “the hidden one” [Olds and Shoshani 1982], and indeed hiding may be one of the rock hyrax's greatest forms of defense, facilitated by tactile feedback through a large distribution of vibrissae.

## Evolutionary considerations of an expanded vibrissal system

Any theory concerning hyrax vibrissae must take into account that all four extant species appear to exhibit vibrissae (based on visual assessment, although no anatomical or immunohistochemical confirmation has been made in any hyrax species prior to the present study). Tree hyraxes (*Dendrohyrax*) are largely nocturnal and – as their name suggests - predominantly live in tree habitats, commonly nesting in the hollows of Hagenia trees [Milner and Harris 1999]. Other terrestrial mammals having non-facial vibrissae are also arboreal, including squirrels [Hyvärinen et al. 1977], with vibrissae presumably providing feedback regarding body position relative to the substrate (tree branches or trunks) [Sokolov

and Kulikov 1987]. All hyrax species are known to be skilled at climbing and jumping [Rubsamen et al. 1982], presumably involving proprioceptive feedback facilitated by vibrissae position on the post-facial body. The yellow-spotted rock hyrax (*Heterohyrac brucei*) habitat consists of boulders, cliffs, and small hills, with this species often occupying the same rock crevices as *Procavia capensis* [Barry and Shoshani 2000; Hoeck 1989] (although minimal overlap in their diets minimizes competition for food resources [Kingdon 1971]). Presumably post-facial vibrissae would confer similar advantages (as described above) navigating these overlapping habitats across rock hyrax species. Beyond feedback related to immediate surroundings (tree hollows, holes in the ground, or rocky crevices), vibrissae also likely provide a sensitive warning system to threats. Since vibrissae extend to a greater length from the body, immediate detection of contact with an object, predator, or conspecific (a high level of intraspecific aggression is present in hyraxes) would allow the hyrax to more quickly flee danger or orient toward it and attack.

Given that hyraxes possess vibrissae in addition to pelage hair on the entire body; that sirenians (manatees and dugongs) exhibit vibrissae on the entire body as the only hair type present [Reep et al. 2002]; and that elephant vibrissae have been discovered on the tip of the trunk [Rasmussen and Munger 1996], but not on the body (Reep, unpublished assessment of histological sections); we can hypothesize that a distributed system of vibrissae on the entire post-facial body, in addition to the face, constitutes the ancestral condition for the supraorder Paenungulata. Across mammalian phylogeny, evidence for the evolution of pelage hair and vibrissae is difficult to trace due to absence of soft tissue in the fossil record, but evidence for hairs can be traced back to multituberculates in the Late Paleocene and hairs are thought to have been present in the most recent common ancestor of multituberculates, monotremes, and therians approximately 210 mya [Meng and Wyss 1997]. Vibrissae are thought to be phylogenetically older than pelage hair [Brink 1956; Estes 1961; Findlay 1968, 1970; Tatarinov 1967; Watson 1931] and generally develop first during ontogeny [Ahl 1986; Davidson and Hardy 1952; Dun 1959; Grüneberg 1943; Klauer et al. 2001; Kollar 1970; Ling 1977]. Maderson [Maderson 2003] proposed that mutations in patterning genes led to multiplication of protovibrissae and protopelage, conferring the selective advantages of protecting the skin from abrasion and enhancing thermoregulation (minimizing cutaneous water loss and providing an insulator barrier). A mutation leading to up-regulation of Wnt/β-catenin is a likely candidate [Dhouailly 2009; Maderson 2003], given that β-catenin causes follicle morphogenesis [Gat et al. 1998; Moore and Lemischka 2006] and Wnt initiates hair follicle development, also helping to determine spacing between hair follicles [Andl et al. 2002; Chang et al. 2004; Gat et al. 1998; Sick et al. 2006]. In addition, *Blimp 1* – a zinc-finger transcriptional repressor – specifically induces vibrissae [Robertson et al. 2007]. Such cell signaling mechanisms point to substrates that were likely to have been modified in Hyracoidea and Sirenia lineages to produce an expanded system of vibrissae, ultimately facilitating navigation of the environment and enhancing survival.

Peripheral specializations that involve dense innervation, such as vibrissae, are reflected by enlarged representations within the central nervous system. Microelectrode mapping of the rock hyrax primary somatosensory cortex mirrors physiological specializations in the periphery by demonstrating enlarged perioral and intraoral representations [Welker and

Carlson 1976]. In fact, 67% of primary somatosensory cortex was taken up by the head representation, an expansion thought to facilitate tactile feedback during grazing on vegetation [Welker and Carlson 1976] similar to sheep [Johnson et al. 1974]. In closely related taxa such as manatees, the perioral region is also believed to be represented by large cortical regions [Marshall and Reep 1995; Reep et al. 1989; Sarko and Reep 2007] further indicating convergent evolutionary paths for Hyracoidea and Sirenia.

## Acknowledgements

The authors would like to sincerely thank Marilyn Dockum and Maggie Stoll for their invaluable technical assistance. The funding for this project was provided by the University of Florida College of Veterinary Medicine to RLR, and NIH grant # NS34692 to FLR.

Funding for this project provided by the University of Florida College of Veterinary Medicine

## Abbreviations

| | |
|---|---|
| **BM** | basement membrane |
| **BNaC** | protein associated with low-threshold mechanoreceptors |
| **BSA** | bovine serum albumin |
| **Cap** | capsule |
| **CGRP** | calcitonin gene-related peptide |
| **CS** | cavernous sinus |
| **DAPI** | 4',6-diamidino-2-phenylindole; nuclear marker |
| **DVN** | deep vibrissal nerve |
| **Epi** | epidermis |
| **FNE** | free nerve ending |
| **FSC** | follicle-sinus complex (vibrissa) |
| **GM** | glassy membrane |
| **HP** | hair papilla |
| **HS** | hair shaft |
| **ICB** | inner conical body |
| **IRS** | inner root sheath |
| **LLE** | longitudinal lanceolate ending |
| **MBP** | myelin basic protein |
| **ME/MEC** | Merkel ending/Merkel ending complex |
| **MR** | mesenchymal ridge |
| **MS** | mesenchymal sheath |
| **mya** | million years ago |

| | |
|---|---|
| **NF or NF200** | 200kD subunit of neurofilament |
| **NPY** | neuropeptide Y |
| **OCB** | outer conical body |
| **ORS** | outer root sheath |
| **PBS** | phosphate buffered saline |
| **PGP** | protein gene product 9.5, a universal neuronal marker and cytoplasmic enzyme |
| **RRC** | rete ridge collar |
| **RS** | ring sinus |
| **RW** | ringwulst |
| **S100** | low-molecular-weight proteins found in vertebrates; Schwaan cell marker |
| **SG** | sebaceous gland |
| **SVN** | superficial vibrissal nerve |
| **TH** | tyrosine hydroxilase |
| **TRB** | trabecula |
| **Ven** | venous supply |
| **TrpV1** | vanilloid receptor 1, capsacin binder |

## References


Ahl AS. The role of vibrissae in behavior: A status review. Vet Res Commun. 1986; 10:245–268. [PubMed: 3526705]

Albrecht PJ, Hines S, Eisenberg E, Pud D, Finlay DR, Connolly MK, Pare M, Davar G, Rice FL. Pathologic alterations of cutaneous innervation and vasculature in affected limbs from patients with complex regional pain syndrome. Pain. 2006; 120:244–266. [PubMed: 16427199]

Andl T, Reddy ST, Gaddapara T, Millar SE. Wnt signals are required for the initiation of hair follicle development. Dev Cell. 2002; 2:643–653. [PubMed: 12015971]

Asher RJ, Novacek MJ, Geisler JH. Relationships of endemic african mammals and their fossil relatives based on morphological and molecular evidence. J Mammal Evol. 2003; 10:131–194.

Barry RE, Shoshani J. Heterohyrax brucei. Mammalian species. 2000; 645:1–7.

Brecht M, Preilowski B, Merzenich MM. Functional architecture of the mystacial vibrissae. Behavioural Brain Research. 1997; 84:81–97. [PubMed: 9079775]

Brink AS. Speculations on some advanced mammalian characteristics in the higher mammal-like reptiles. Paleontol Afr. 1956; 4:77–96.

Brown KJ, Downs CT. Seasonal patterns in body temperature of free-living rock hyrax (procavia capensis). Comparative biochemistry and physiology Part A, Molecular & integrative physiology. 2006; 143:42–49.

Bryden MM, Marsh H, Macdonald BW. Skin and hair of dugong, dugong-dugon. Journal of anatomy. 1978; 126:637–638.

Burgess, PR.; Perl, ER. Cutaneous mechanoreceptors and nociceptors.. In: Iggo, A., editor. Handbook of sensory physiology, 2, somatosensory systems. Springer-Verlag; Berlin: 1973. p. 29-78.

Chang CH, Jiang TX, Lin CM, Burrus LW, Chuong CM, Widelitz R. Distinct wnt members regulate the hierarchical morphogenesis of skin regions (spinal tract) and individual feathers. Mech Dev. 2004; 121:157–171. [PubMed: 15037317]

Coe MJ. Notes on the habits of the mount kenya hyrax (procavia johnstoni mackinderi). Proc Zool Soc Lond. 1962; 138:639–644.

Cooper LN, Seiffert ER, Clementz M, Madar SI, Bajpai S, Hussain ST, Thewissen JG. Anthracobunids from the middle eocene of india and pakistan are stem perissodactyls. PloS one. 2014; 9:e109232. [PubMed: 25295875]

Crandall, LS. The management of wild mammals in captivity. University of Chicago Press; Chicago: 1964.

Crish SD, Rice FL, Park TJ, Comer CM. Somatosensory organization and behavior in naked mole-rats i: Vibrissa-like body hairs comprise a sensory array that mediates orientation to tactile stimuli. Brain Behavior and Evolution. 2003; 62:141–151.

Czech-Damal NU, Liebschner A, Miersch L, Klauer G, Hanke FD, Marshall C, Dehnhardt G, Hanke W. Electroreception in the guiana dolphin (sotalia guianensis). Proceedings Biological sciences / The Royal Society. 2012; 279:663–668. [PubMed: 21795271]

Czech-Damal NU, Dehnhardt G, Manger P, Hanke W. Passive electroreception in aquatic mammals. Journal of comparative physiology A, Neuroethology, sensory, neural, and behavioral physiology. 2013; 199:555–563.

Davidson P, Hardy MH. The development of mouse vibrissae in vivo and in vitro. Journal of anatomy. 1952; 86:342–356. [PubMed: 12999638]

de Jong WW. Molecules remodel the mammalian tree. Trends in ecology & evolution. 1998; 13:270–275. [PubMed: 21238296]

Dehnhardt G, Hyvarinen H, Palviainen A, Klauer G. Structure and innervation of the vibrissal follicle-sinus complex in the australian water rat, hydromys chrysogaster. The Journal of comparative neurology. 1999; 411:550–562. [PubMed: 10421867]

Dehnhardt G, Mauck B, Hanke W, Bleckmann H. Hydrodynamic trail-following in harbor seals (phoca vitulina). Science. 2001; 293:102–104. [PubMed: 11441183]

Dhouailly D. A new scenario for the evolutionary origin of hair, feather, and avian scales. Journal of anatomy. 2009; 214:587–606. [PubMed: 19422430]

Dosch F. Structure and development of the integument of sirenia. Tech. Trans. No. 1626. National research council of canada, ottawa, 1973. Jenaische Zeitschr. 1915; 53:805–854.

Dun RB. The development and growth of vibrissae in the house mouse with particular reference to the time of action of the tabby (ta) and ragged (ra) genes. Aust J Biol Sci. 1959; 12:312–339.

Ebara S, Kumamoto K, Matsuura T, Mazurkiewicz JE, Rice FL. Similarities and differences in the innervation of mystacial vibrissal follicle-sinus complexes in the rat and cat: A confocal microscopic study. The Journal of comparative neurology. 2002; 449:103–119. [PubMed: 12115682]

Eisenberg, JF. The mammalian radiations. University of Chicago Press; Chicago: 1981.

Estes FR. Cranial anatomy of the cynodont reptile *thrinaxodon liothinus*. Bulletin of the Museum of Comparative Zoology. 1961; 125:165–180.

Fairall N, Eloff AK, McNairn IS. Integration of metabolism and digestion in the hyrax. S Afr J Anim Sci. 1983; 13:79–80.

Findlay GH. On the scalasaurid skull of oliveieria paringtoni, brink with a note on the origin of hair. Paleontol Afr. 1968; 11:47–59.

Findlay GH. The role of skin in the origin of mammals. S Afr J Sci. 1970; 66:277–283.

Fourie PB. Acoustic communication in the rock hyrax *procavia capensis*. Z Tierpsychol. 1977; 44:194–219.

Fundin BT, Arvidsson J, Rice FL. Innervation of nonmystacial vibrissae in the adult rat. The Journal of comparative neurology. 1995; 357:501–512. [PubMed: 7673481]

Fundin BT, Pfaller K, Rice FL. Different distributions of the sensory and autonomic innervation among the microvasculature of the rat mystacial pad. The Journal of comparative neurology. 1997a; 389:545–568. [PubMed: 9421138]

Fundin BT, Silos-Santiago I, Ernfors P, Fagan AM, Aldskogius H, DeChiara TM, Phillips HS, Barbacid M, Yancopoulos GD, Rice FL. Differential dependency of cutaneous mechanoreceptors on neurotrophins, trk receptors, and p75 lngfr. Developmental biology. 1997b; 190:94–116. [PubMed: 9331334]

Garcia-Anoveros J, Samad TA, Zuvela-Jelaska L, Woolf CJ, Corey DP. Transport and localization of the deg/enac ion channel bnac1alpha to peripheral mechanosensory terminals of dorsal root ganglia neurons. The Journal of neuroscience : the official journal of the Society for Neuroscience. 2001; 21:2678–2686. [PubMed: 11306621]

Gat U, DasGupta R, Degenstein L, Fuchs E. De novo hair follicle morphogenesis and hair tumors in mice expressing a truncated beta-catenin in skin. Cell. 1998; 95:605–614. [PubMed: 9845363]

Gheerbrant E. Paleocene emergence of elephant relatives and the rapid radiation of african ungulates. Proceedings of the National Academy of Sciences of the United States of America. 2009; 106:10717–10721. [PubMed: 19549873]

Ginter CC, DeWitt TJ, Fish FE, Marshall CD. Fused traditional and geometric morphometrics demonstrate pinniped whisker diversity. PloS one. 2012; 7:e34481. [PubMed: 22509310]

Gottschaldt KM, Iggo A, Young DW. Functional characteristics of mechanoreceptors in sinus hair follicles of the cat. The Journal of physiology. 1973; 235:287–315. [PubMed: 4763992]

Gottschaldt KM, Vahle-Hinz C. Merkel cell receptors: Structure and transducer function. Science. 1981; 214:183–186. [PubMed: 7280690]

Grüneberg H. The development of some external features in mouse embryos. Journal of Heredity. 1943; 34:89–92.

Hoeck HN. Differential feeding behavior of the sypatric hyrax, *procavia johnstoni* and *heterohyrax brucei*. Oecologia. 1975; 22:15–47.

Hoeck HN. Demography and competition in hyrax: A 17 year study. Oecologia. 1989; 79:353–360. [PubMed: 23921400]

Hvass, H. Mammals of the world. Methuen; London: 1961.

Hyvärinen H, Kangasperko H, Peura R. Functional structure of the carpal and ventral vibrissae of the squirrel (sciurus vulgaris). Journal of Zoology. 1977; 182:457–466.

Iggo A. New specific sensory structure in hairy skin. Acta Neuroveg (Wien). 1963; 24:175–180.

Iggo, A. Cutaneous receptors with a high sensitivity to mechanical displacement.. In: de Reuck, AVS.; Knight, J., editors. Touch, heat and pain. Churchill; London: 1966. p. 237-256.

Iggo A, Muir AR. The structure and function of a slowly adapting touch corpuscle in hairy skin. The Journal of physiology. 1969; 200:763–796. [PubMed: 4974746]

Johansson AS, Vallbo AB. Tactile sensory coding in the glabrous skin od the human hand. TINS. 1983; 6:27–32.

Johansson RS, Landstrom U, Lundstrom R. Sensitivity to edges of mechanoreceptive afferent units innervating the glabrous skin of the human head. Brain research. 1982a; 244:27–35. [PubMed: 6288181]

Johansson RS, Landstrom U, Lundstrom R. Responses of mechanoreceptive afferent units in the glabrous skin of the human hand to sinusoidal skin displacements. Brain research. 1982b; 244:17–25. [PubMed: 6288178]

Johnson JI, Rubel EW, Hatton GI. Mechanosensory projections to cerebral cortex of sheep. The Journal of comparative neurology. 1974; 158:81–107. [PubMed: 4430738]

Kamiya, T.; Yamasaki, F. A morphological note on the sinus hair of the dugong.. In: Marsh, H., editor. The dugong. Dept. of Zoology, James Cook University of North Queensland; Australia: 1981. p. 111-113.

Kellogg ME, Burkett S, Dennis TR, Stone G, Gray BA, McGuire PM, Zori RT, Stanyon R. Chromosome painting in the manatee supports afrotheria and paenungulata. BMC evolutionary biology. 2007; 7:6. [PubMed: 17244368]

Kemp, TS. The origin and evolution of mammals. Oxford University Press; New York: 2005. Living and fossil placentals.; p. 222-257.

Kingdon, J. An atlas of evolution in africa. Vol. 1. Academic Press; New York: 1971. East african mammals.; p. 329-351.

Klauer GJ, Bachteler D, Drees E, Hilken G. Vibrissae - more than just hairs! Journal of morphology. 2001; 248:248–249.

Kleinschmidt T, Czelusniak J, Goodman M, Braunitzer G. Paenungulata: A comparison of the hemoglobin sequences from elephant, hyrax, and manatee. Molecular biology and evolution. 1986; 3:427–435. [PubMed: 3444412]

Kollar EJ. The induction of hair follicles by embryonic dermal papillae. J Invest Dermatol. 1970; 55:374–378. [PubMed: 5489079]

Lavergne A, Douzery E, Stichler T, Catzeflis FM, Springer MS. Interordinal mammalian relationships: Evidence for paenungulate monophyly is provided by complete mitochondrial 12s rrna sequences. Molecular phylogenetics and evolution. 1996; 6:245–258. [PubMed: 8899726]

Layne JN, Caldwell DK. Behavior of the amazon dolphin, inia geoffrensis (blainville), in captivity. Zoologica. 1964; 49:81–108.

Lichtenstein SH, Carvell GE, Simons DJ. Responses of rat trigeminal ganglion neurons to movements of vibrissae in different directions. Somatosensory & motor research. 1990; 7:47–65. [PubMed: 2330787]

Ling, JK. Vibrissae of marine mammals.. In: Harrison, RJ., editor. Functional anatomy of marine mammals. Vol. 3. Academic Press; London: 1977. p. 387-415.

Liu FG, Miyamoto MM, Freire NP, Ong PQ, Tennant MR, Young TS, Gugel KF. Molecular and morphological supertrees for eutherian (placental) mammals. Science. 2001; 291:1786–1789. [PubMed: 11230694]

Maderson PF. Mammalian skin evolution: A reevaluation. Experimental dermatology. 2003; 12:233–236. [PubMed: 12823435]

Marshall CD, Reep RL. Manatee cerebral cortex: Cytoarchitecture of the caudal region in trichechus manatus latirostris. Brain, behavior and evolution. 1995; 45:1–18.

Marshall CD, Huth GD, Edmonds VM, Halin DL, Reep RL. Prehensile use of perioral bristles during feeding and associated behaviors of the florida manatee (trichechus manatus latirostris). Marine Mammal Science. 1998; 14:274–289.

Marshall CD, Amin H, Kovacs KM, Lydersen C. Microstructure and innervation of the mystacial vibrissal follicle-sinus complex in bearded seals, erignathus barbatus (pinnipedia: Phocidae). The anatomical record Part A, Discoveries in molecular, cellular, and evolutionary biology. 2006; 288:13–25.

Meng J, Wyss AR. Multituberculate and other mammal hair recovered from palaeogene excreta. Nature. 1997; 385:712–714. [PubMed: 9034186]

Mercado E III. Tubercles: What sense is there? Aquatic Mammals. 2014; 40:95–103.

Miller EH. A comparative study of facial expressions of two species of pinnipeds. Behaviour. 1975; 53:268–284.

Milner JM, Harris S. Habitat use and ranging behavior of tree hyrax, *dendorhyrax arboreus*, in the virginia volcanoes, rwanda. African Journal of Ecology. 1999; 37:281–294.

Moore BW. A soluble protein characteristic of the nervous system. Biochemical and biophysical research communications. 1965; 19:739–744. [PubMed: 4953930]

Moore BW. Chemistry and biology of the s-100 protein. Scandinavian journal of immunology Supplement. 1982; 9:53–74. [PubMed: 6190220]

Moore KA, Lemischka IR. Stem cells and their niches. Science. 2006; 311:1880–1885. [PubMed: 16574858]

Munger BL, Pubols LM, Pubols BH. The merkel rete papilla--a slowly adapting sensory receptor in mammalian glabrous skin. Brain research. 1971; 29:47–61. [PubMed: 5564262]

Murata Y, Nikaido M, Sasaki T, Cao Y, Fukumoto Y, Hasegawa M, Okada N. Afrotherian phylogeny as inferred from complete mitochondrial genomes. Molecular phylogenetics and evolution. 2003; 28:253–260. [PubMed: 12878462]

Nishihara H, Maruyama S, Okada N. Retroposon analysis and recent geological data suggest near-simultaneous divergence of the three superorders of mammals. Proceedings of the National Academy of Sciences of the United States of America. 2009; 106:5235–5240. [PubMed: 19286970]

Olds N, Shoshani J. Procavia capensis. Mammalian species. 1982; 171:1–7.

Ozawa T, Hayashi S, Mikhelson VM. Phylogenetic position of mammoth and steller's sea cow within tethytheria demonstrated by mitochondrial DNA sequences. Journal of molecular evolution. 1997; 44:406–413. [PubMed: 9089080]

Pardini AT, O'Brien PC, Fu B, Bonde RK, Elder FF, Ferguson-Smith MA, Yang F, Robinson TJ. Chromosome painting among proboscidea, hyracoidea and sirenia: Support for paenungulata (afrotheria, mammalia) but not tethytheria. Proceedings Biological sciences / The Royal Society. 2007; 274:1333–1340. [PubMed: 17374594]

Pare M, Elde R, Mazurkiewicz JE, Smith AM, Rice FL. The meissner corpuscle revised: A multiafferented mechanoreceptor with nociceptor immunochemical properties. The Journal of neuroscience : the official journal of the Society for Neuroscience. 2001; 21:7236–7246. [PubMed: 11549734]

Pare M, Smith AM, Rice FL. Distribution and terminal arborizations of cutaneous mechanoreceptors in the glabrous finger pads of the monkey. The Journal of comparative neurology. 2002; 445:347–359. [PubMed: 11920712]

Park TJ, Comer C, Carol A, Lu Y, Hong HS, Rice FL. Somatosensory organization and behavior in naked mole-rats: Ii. Peripheral structures, innervation, and selective lack of neuropeptides associated with thermoregulation and pain. The Journal of comparative neurology. 2003; 465:104–120. [PubMed: 12926019]

Pocock RI. On the facial vibrissae of mammalia. J Zool (London). 1914; 84:889–912.

Rasmussen LE, Munger BL. The sensorineural specializations of the trunk tip (finger) of the asian elephant, elephas maximus. The Anatomical record. 1996; 246:127–134. [PubMed: 8876831]

Reep RL, Johnson JI, Switzer RC, Welker WI. Manatee cerebral cortex: Cytoarchitecture of the frontal region in trichechus manatus latirostris. Brain, behavior and evolution. 1989; 34:365–386.

Reep RL, Marshall CD, Stoll ML, Whitaker DM. Distribution and innervation of facial bristles and hairs in the florida manatee (trichechus manatus latirostris). Marine Mammal Science. 1998; 14:257–273.

Reep RL, Stoll ML, Marshall CD, Homer BL, Samuelson DA. Microanatomy of facial vibrissae in the florida manatee: The basis for specialized sensory function and oripulation. Brain, behavior and evolution. 2001; 58:1–14.

Reep RL, Marshall CD, Stoll ML. Tactile hairs on the postcranial body in florida manatees: A mammalian lateral line? Brain Behavior and Evolution. 2002; 59:141–154.

Rice FL, Mance A, Munger BL. A comparative light microscopic analysis of the sensory innervation of the mystacial pad. I. Innervation of vibrissal follicle-sinus complexes. The Journal of comparative neurology. 1986; 252:154–174. [PubMed: 3782505]

Rice FL, Fundin BT, Arvidsson J, Aldskogius H, Johansson O. Comprehensive immunofluorescence and lectin binding analysis of vibrissal follicle sinus complex innervation in the mystacial pad of the rat. The Journal of comparative neurology. 1997; 385:149–184. [PubMed: 9268122]

Rice FL, Rasmusson DD. Innervation of the digit on the forepaw of the raccoon. The Journal of comparative neurology. 2000; 417:467–490. [PubMed: 10701867]

Roberts, A. The mammals of south africa. Central News Agency; South Africa: 1951.

Robertson EJ, Charatsi I, Joyner CJ, Koonce CH, Morgan M, Islam A, Paterson C, Lejsek E, Arnold SJ, Kallies A, Nutt SL, Bikoff EK. Blimp1 regulates development of the posterior forelimb, caudal pharyngeal arches, heart and sensory vibrissae in mice. Development. 2007; 134:4335–4345. [PubMed: 18039967]

Rosenfeld MG, Mermod JJ, Amara SG, Swanson LW, Sawchenko PE, Rivier J, Vale WW, Evans RM. Production of a novel neuropeptide encoded by the calcitonin gene via tissue-specific rna processing. Nature. 1983; 304:129–135. [PubMed: 6346105]

Rubsamen K, Hume ID, Engelhardt WV. Physiology of the rock hyrax. Comparative biochemistry and physiology Part A, Molecular & integrative physiology. 1982; 72A:271–277.

Ruiz-Herrera A, Robinson TJ. Chromosomal instability in afrotheria: Fragile sites, evolutionary breakpoints and phylogenetic inference from genome sequence assemblies. BMC evolutionary biology. 2007; 7:199. [PubMed: 17958882]

Sale JB. The habitat of the rock hyrax. JE Africa Nat Hist Soc. 1966; 25:205–214.

Sale JB. Unusual external adaptations in the rock hyrax. Zool Afr. 1970a; 5:101–113.

Sale JB. The behaviour of the resting rock hyrax in relation to its environment. Zool Africana. 1970b; 5:87–99.

Sarko DK, Reep RL. Somatosensory areas of manatee cerebral cortex: Histochemical characterization and functional implications. Brain, behavior and evolution. 2007; 69:20–36.

Sarko DK, Reep RL, Mazurkiewicz JE, Rice FL. Adaptations in the structure and innervation of follicle-sinus complexes to an aquatic environment as seen in the florida manatee (trichechus manatus latirostris). The Journal of comparative neurology. 2007; 504:217–237. [PubMed: 17640045]

Sarko DK, Rice FL, Reep RL. Mammalian tactile hair: Divergence from a limited distribution. Annals of the New York Academy of Sciences. 2011; 1225:90–100. [PubMed: 21534996]

Shortridge, GC. The mammals of southwest africa. Vol. 1. William Heinemann, Ltd; 1934. p. 380-384.

Shoshani J, McKenna MC. Higher taxonomic relationships among extant mammals based on morphology, with selected comparisons of results from molecular data. Molecular phylogenetics and evolution. 1998; 9:572–584. [PubMed: 9668007]

Shoshani, J. Order hyracoidea.. In: Wilson, DE.; Reeder, DM., editors. Mammal species of the world. Johns Hopkins University Press; 2005. p. 87-88.

Sick S, Reinker S, Timmer J, Schlake T. Wnt and dkk determine hair follicle spacing through a reaction-diffusion mechanism. Science. 2006; 314:1447–1450. [PubMed: 17082421]

Simpson GG. The principles of classification and a classification of mammals. Bulletin of the American Museum of Natural History. 1945; 85:1–350.

Sokolov VE, Sale JB. The structure of skin in the hyracoidea (mammalia). Part 1. Zoologicheskii Zhurnal. 1981a; 60:1695–1703.

Sokolov VE, Sale JB. The structure of skin in the hracoidea (mammalia). Part 2. Zoologicheskii Zhurnal. 1981b; 60:1849–1860.

Sokolov, VE. Mammal skin. University of California Press; Berkeley, CA: 1982.

Sokolov, VE. Manatee - morphological description. Nauka Press; Moscow: 1986.

Sokolov VE, Kulikov VF. The structure and function of the vibrissal apparatus in some rodents. Mammalia. 1987; 51:125–138.

Springer MS, Cleven GC, Madsen O, de Jong WW, Waddell VG, Amrine HM, Stanhope MJ. Endemic african mammals shake the phylogenetic tree. Nature. 1997; 388:61–64. [PubMed: 9214502]

Springer MS, Murphy WJ, Eizirik E, O'Brien SJ. Placental mammal diversification and the cretaceous-tertiary boundary. Proceedings of the National Academy of Sciences of the United States of America. 2003; 100:1056–1061. [PubMed: 12552136]

Springer MS, Stanhope MJ, Madsen O, de Jong WW. Molecules consolidate the placental mammal tree. Trends in ecology & evolution. 2004; 19:430–438. [PubMed: 16701301]

Stefansson K, Wollmann RL, Moore BW. Distribution of s-100 protein outside the central nervous system. Brain research. 1982; 234:309–317. [PubMed: 7059833]

Stoddart DM, Fairall N. Electrocardiographic technique for studying olfactory response in the rock hyraxprocavia capensis l. (mammalia: Hyracoidea). Journal of chemical ecology. 1981; 7:257–263. [PubMed: 24420471]

Tatarinov LP. Development of the system of labial (vibrissal) vessels and nerves in theriodonts. Paleontol Zh. 1967; 1:3–17.

Tuckett RP. Response of cutaneous hair and field mechanoreceptors in cat to paired mechanical stimuli. Journal of neurophysiology. 1978; 41:150–156. [PubMed: 621541]

Tuckett RP, Horch KW, Burgess PR. Response of cutaneous hair and field mechanoreceptors in cat to threshold stimuli. Journal of neurophysiology. 1978; 41:138–149. [PubMed: 621540]

Turner MIM, Watson RM. An introductory study on the ecology of hyrax (*dendrohyrax bruicei* and *procavia johnstoni*) in the serengeti national park. E Afr Wildl J. 1965; 3:49–60.

Walker, EP.; Warnick, F.; Lange, KI.; Vible, HE.; Hamlet, SE.; Davis, MA.; Wright, PF. Mammals of the world. Hopkins Press; Baltimore: 1964.

Watson DMS. On the skeleton of a bauriomorph reptile. Proceedings of the Zoological Society of London. 1931:1163–1205.

Welker WI, Carlson M. Somatic sensory cortex of hyrax (procavia). Brain, behavior and evolution. 1976; 13:294–301.

Wilkinson KD, Lee KM, Deshpande S, Duerksen-Hughes P, Boss JM, Pohl J. The neuron-specific protein pgp 9.5 is a ubiquitin carboxyl-terminal hydrolase. Science. 1989; 246:670–673. [PubMed: 2530630]

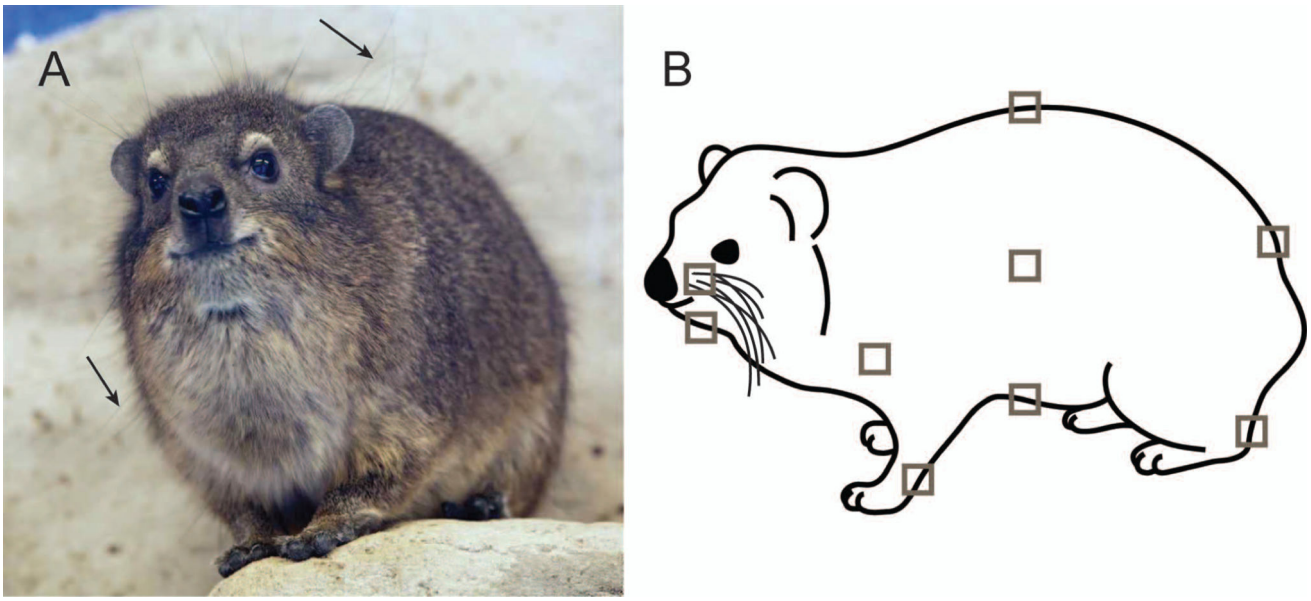


**Figure 1.**

A) Image of a rock hyrax with post-facial vibrissae present as long, black hairs (arrows) dispersed among shorter pelage hair. Picture © Tony Northrup 2014. B) Body regions sampled for follicle-sinus complexes included, from rostral to caudal: mystacial, submental, shoulder, and carpal; dorsal, lateral, and ventral aspects of the mid-region; and both caudal and tarsal regions (nomenclature follows [Sokolov and Kulikov 1987].

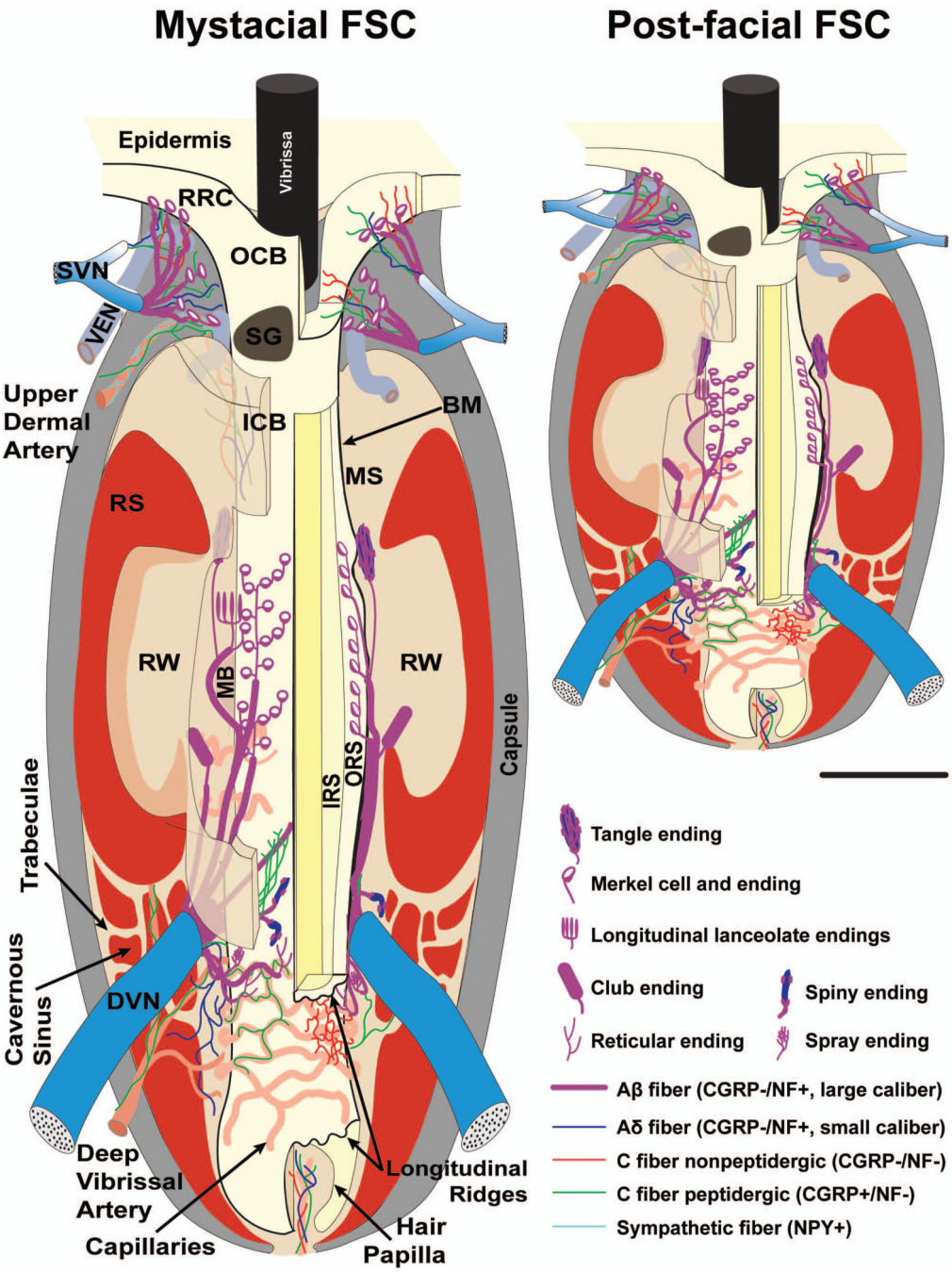


**Figure 2.**

Schematic illustration of representative mystacial and post-facial hyrax follicle-sinus complexes (FSCs) characterizing innervation types and sensory nerve endings observed. Labels for mystacial FSC also apply to post-facial FSC. Each is characterized by a dense connective tissue capsule, dense innervation (particularly Merkel ending complexes), a circumferential ring sinus, a prominent ringwulst, and a dense mesenchymal sheath. The vibrissa of the mystacial FSC (but not the postfacial FSC) exhibited a ridged appearance at the level of the lower ring sinus continuing through the majority of the cavernous sinus. The

relative scale of each FSC is approximately accurate, but innervation is disproportionately scaled to optimize visualization. Scale bar = 1mm. BM = basement membrane, DVN = deep vibrissal nerve, ICB = inner conical body, IRS = inner root sheath, MB = mesenchymal bulge, MS = mesenchymal sheath, OCB = outer conical body, ORS = outer root sheath, RRC = rete ridge collar, RS = ring sinus, RW = ringwulst, SG = sebaceous gland, SVN = superficial vibrissal nerve, VEN = venous supply.

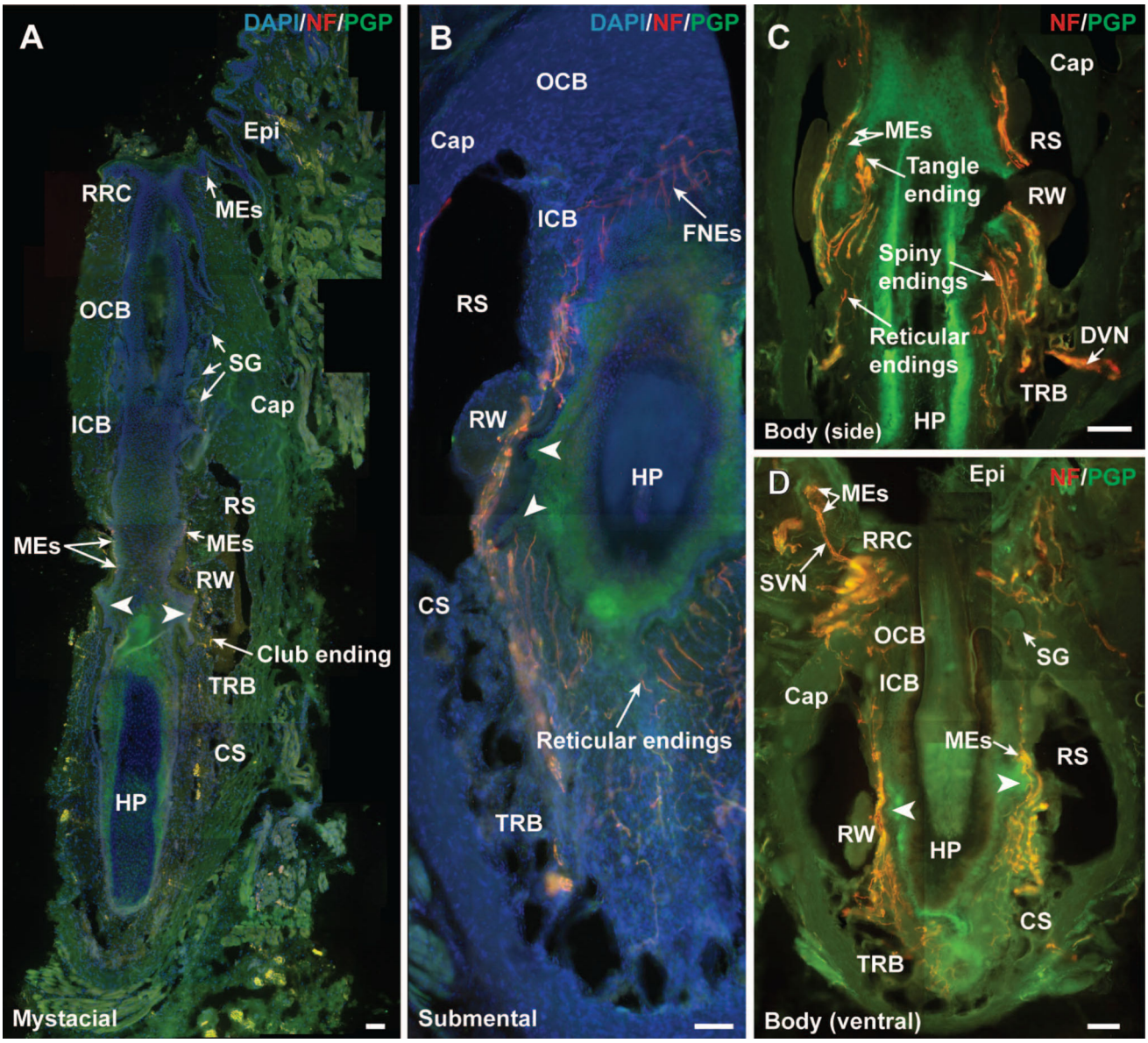


**Figure 3.**

Longitudinal sections just off of the central axis of rock hyrax FSCs illustrating the overall structure, prominent ring sinus and ringwulst, and types of nerve endings present in facial and post-facial body regions. A) mystacial, B) submental, C) lateral body, and D) ventral body region FSCs exhibit the characteristics of true vibrissae. Arrowheads indicate mesenchymal bulges at the ring sinus level. Immunolabeling shown consisted of DAPI (blue, nuclear marker; 4',6-diamidino-2-phenylindole), NF200 (red; 200kD subunit of neurofilament), and PGP (green, universal neuronal marker; protein gene product 9.5). Scale bars=300μm (A-D). Cap = capsule, CS = cavernous sinus, Epi = epidermis, FNEs = free nerve endings, HP = hair papilla, ICB = inner conical body, MEs = Merkel endings, OCB = outer conical body, RRC = rete ridge collar, RS = ring sinus, RW = ringwulst, SG = sebaceous gland, TRB = trabeculae.

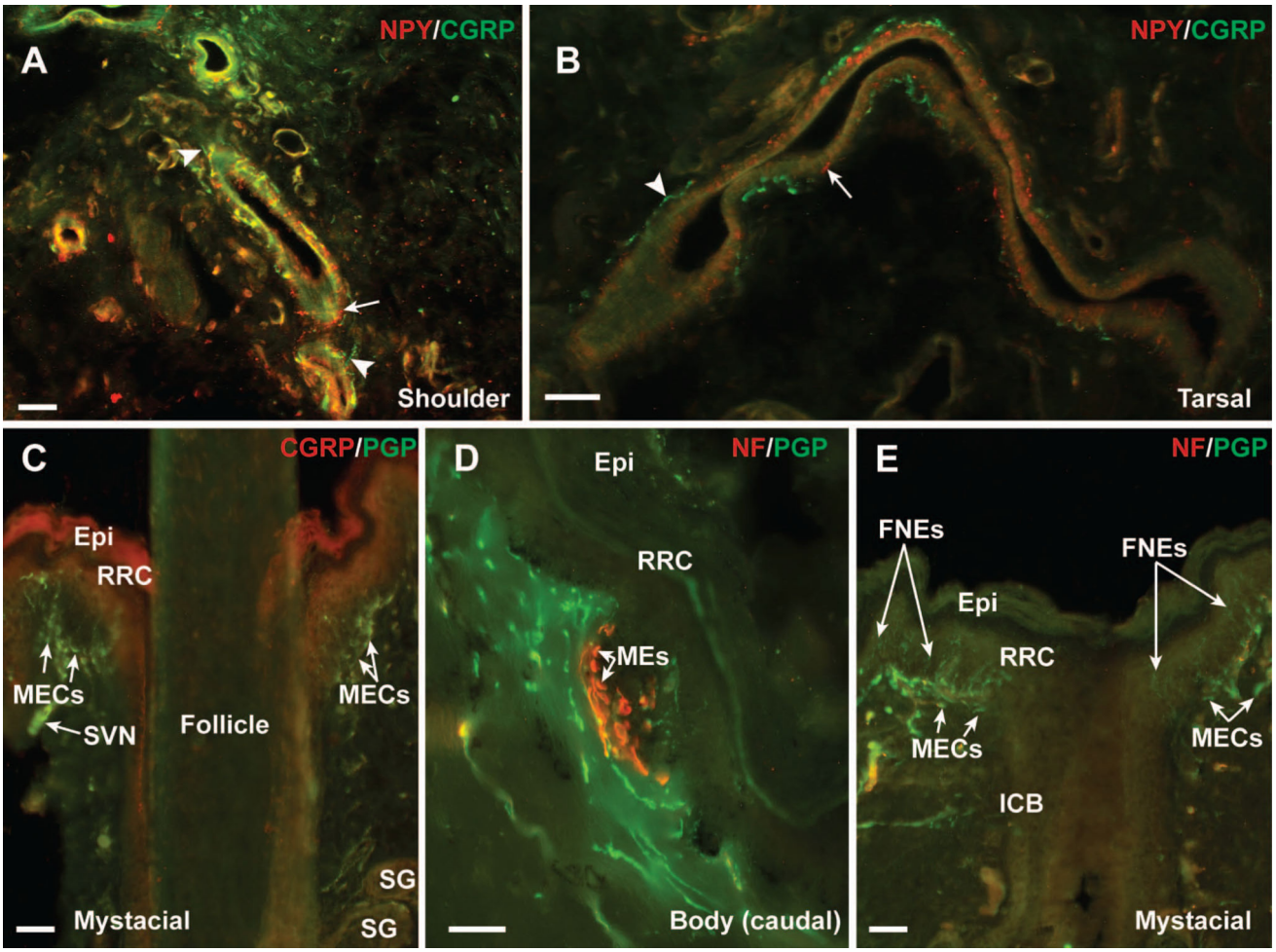


**Figure 4.**

Representative innervation of rock hyrax FSCs at the dermal, rete ridge collar, outer and inner conical body levels. A-B) Innervation associated with upper dermal arteries included sympathetic innervation (NPY+, indicated by arrows) and C-fiber innervation (CGRP+, indicated by arrowheads). C) Innervation at the rete ridge collar (RRC) and epidermal (Epi) level (representative mystacial follicle-sinus complex shown), including bilateral bulges of Merkel ending complexes (MECs) seen as terminations of Aβ fibers from the superficial vibrissal nerve (SVN; seen in more detail in D). Prominent sebaceous glands (SGs) were also observed. E) In addition to MECs, representative innervation at the RRC and inner conical body (ICB) levels included fine-caliber innervation consisting of C- and Aδ-fibers (NF200− and NF200+, respectively) terminating as presumptive free nerve endings (FNEs) in a mystacial follicle-sinus complex. Scale bars=150μm. Epi = epidermis, FNE = free nerve ending, ICB = inner conical body, MEC = Merkel ending complexes, RRC = rete ridge collar, SG = sebaceous gland, SVN = superficial vibrissal nerve. Immunolabeling shown consisted of NPY (red; neuropeptide Y, sympathetic innervation marker) paired with CGRP (green; calcitonin gene-related peptide) (A-B); or CGRP (red) or NF200 (red; 200kD subunit of neurofilament) paired with PGP (green, universal neuronal marker; protein gene product 9.5) (C-E).

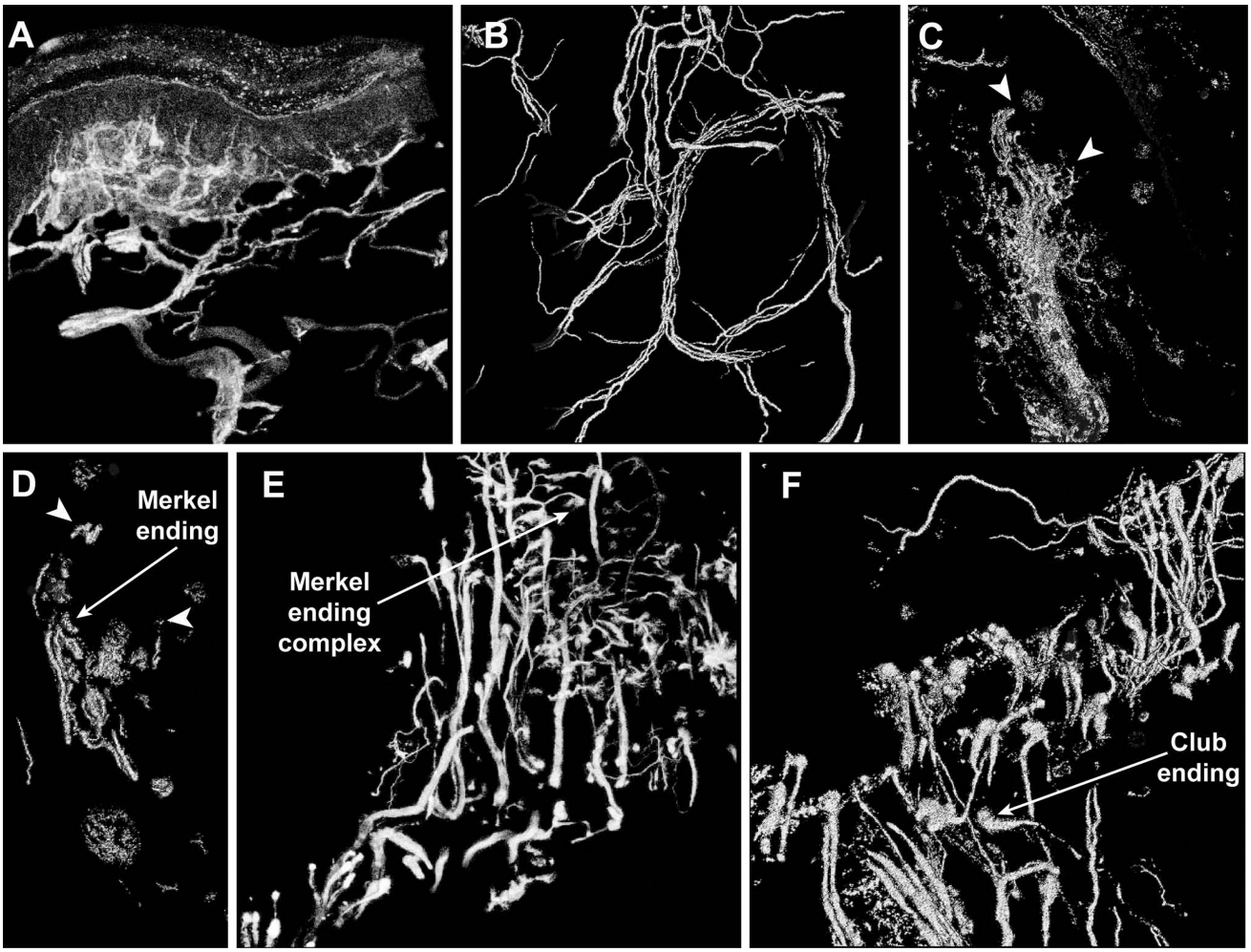


**Figure 5.**

Confocal surface reconstructions illustrating the three-dimensional structure of representative hyrax follicle-sinus complex (FSC) innervation and mechanoreceptors. A) Epidermal and rete ridge collar (RRC) innervation, including small-caliber fibers and Merkel endings (submental FSC). B) Small-caliber innervation at the level of the inner conical body (mystacial FSC). C-D) Semicircular cusp of Merkel innervation at the level of the rete ridge collar (mystacial FSC). Arrowheads demarcate edges of the Merkel complex cusp. E) Extensive large-caliber innervation and Merkel endings at the level of the ring sinus (mystacial FSC). F) Large-caliber innervation and club endings at the level of the ring sinus (mystacial FSC). Immunolabeling shown consisted of PGP (universal neuronal marker; protein gene product 9.5).

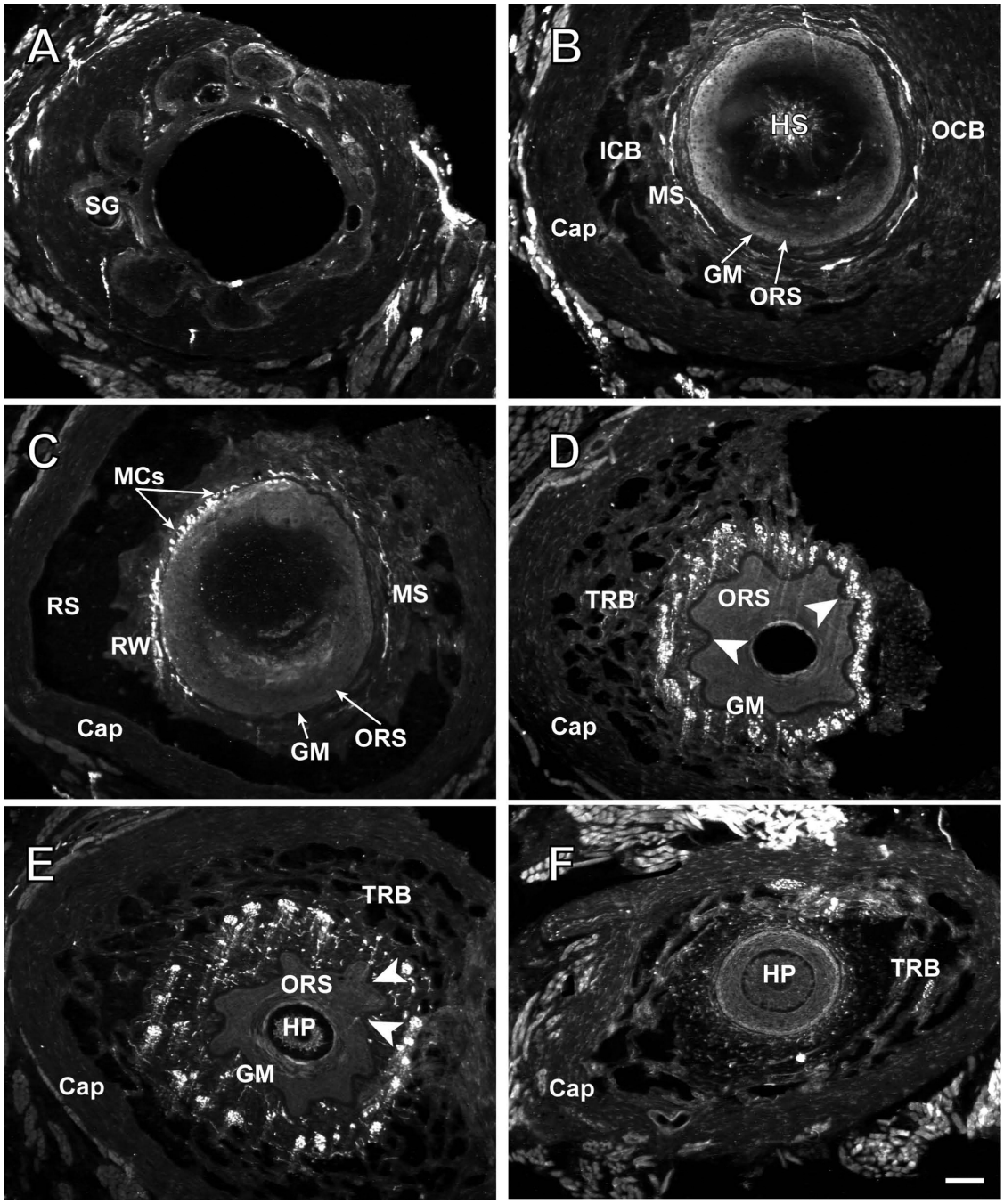


**Figure 6.**

Cross-sectional series from a hyrax mystacial follicle-sinus complex, from superficial to deep levels (A-F). Prominent sebaceous glands are evident (A) and a dense connective tissue capsule surrounds the follicle and its affiliated dense innervation (B-F). Dense Merkel cell innervation can be seen at the ring sinus level surrounding the follicle circumferentially and terminating within the outer root sheath (C). The irregular morphology of the hair follicle becomes apparent at the lower ring sinus and cavernous sinus levels where prominent longitudinal ridges appear (white arrowheads; D-E), and an absence of lateral innervation

(within the trabeculae) at the cavernous sinus level is evident (D-F). Immunolabeling shown consisted of PGP (universal neuronal marker; protein gene product 9.5). Scale bar = 300μm (A-F). Cap=capsule, GM=glassy membrane, HP=hair papilla, HS = hair shaft, ICB=inner conical body, MCs=Merkel cells, MS=mesenchymal sheath, OCB=outer conical body, ORS=outer root sheath, RS=ring sinus, RW=ringwulst, SG=sebaceous gland, TRB=trabeculae.

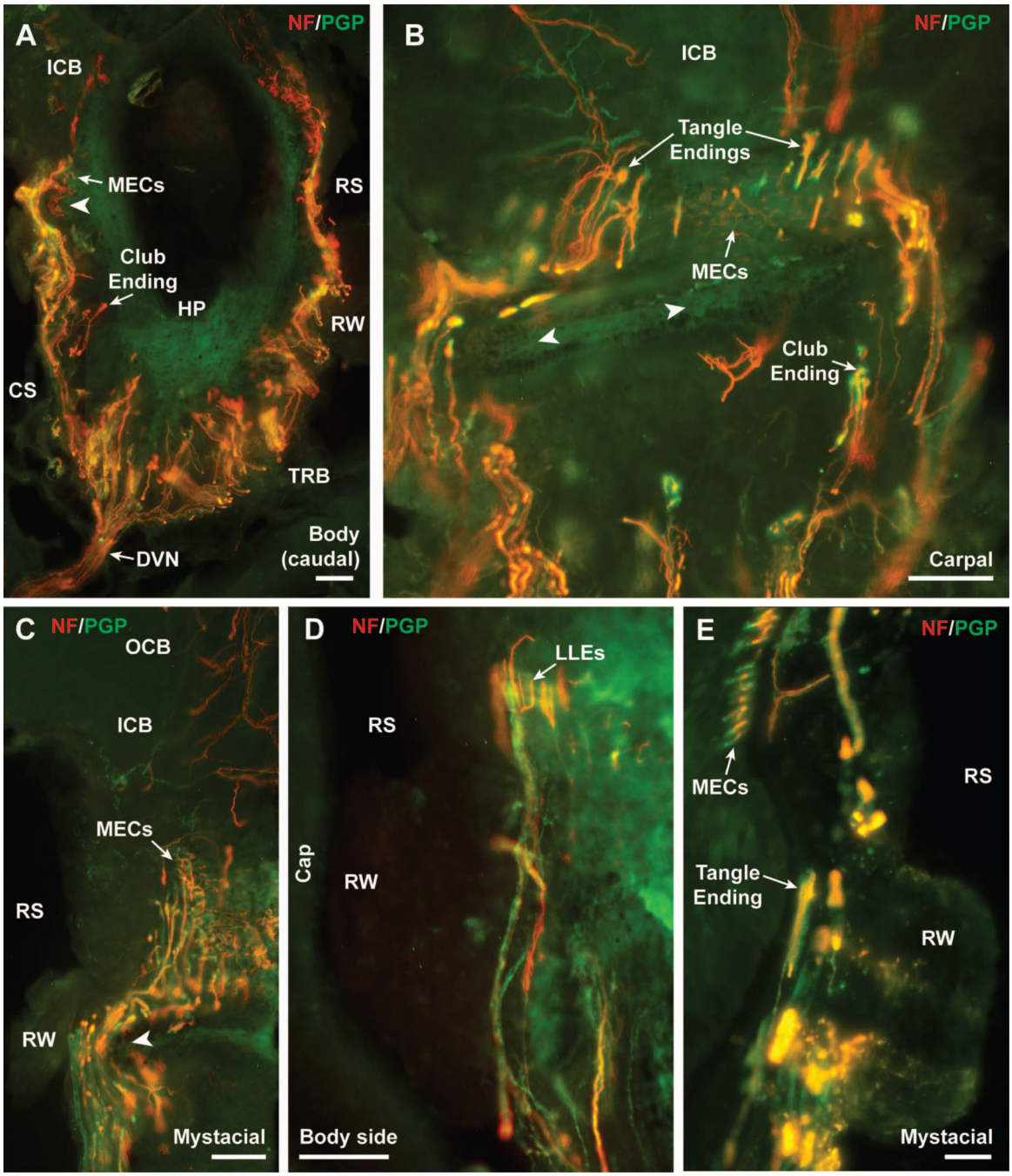


**Figure 7.**

Characterization of hyrax follicle-sinus complex (FSC) innervation at the ring sinus (RS) level (longitudinal planes of section). A) Characteristic innervation at the RS and cavernous sinus (CS) levels of a representative follicle-sinus complex from the caudal body. Arrowhead denotes a mesenchymal bulge at the ring sinus level in proximity to the ringwulst (RW). Large-caliber fibers from the deep vibrissal nerve (DVN) can be seen ascending superficially through the cavernous sinus, curving around the mesenchymal bulge to terminate as Merkel ending complexes (MECs). B) At the level of the ring sinus, club

endings and MEC networks can be observed. A mesenchymal bulge at the ring sinus level in proximity to the ringwulst is visible (arrowheads), and presumptive “tangle” endings are apparent at the upper RS/lower ICB level as terminations of large-caliber fibers. C) Fine-caliber innervation is observed at the outer and inner conical body levels, whereas the ring sinus is characterized by dense, circumferential networks of MECs. The mesenchymal bulge proximal to the ringwulst is denoted by the arrowhead. D) Longitudinal lanceolate endings were present along the mesenchymal sheath at the upper extent of the ring sinus, but were relatively sparsely distributed. E) MECs terminate in the outer root sheath of the follicle at the ring sinus level, and large tangle endings were observed. Scale bars=300μm (A-D), 75μm (E). Cap = capsule, CS = cavernous sinus, DVN = deep vibrissal nerve, HP = hair papilla, ICB = inner conical body, LLEs = longitudinal lanceolate endings, MECs = Merkel ending complexes, OCB = outer conical body, RS = ring sinus, RW = ringwulst, TRB = trabeculae.

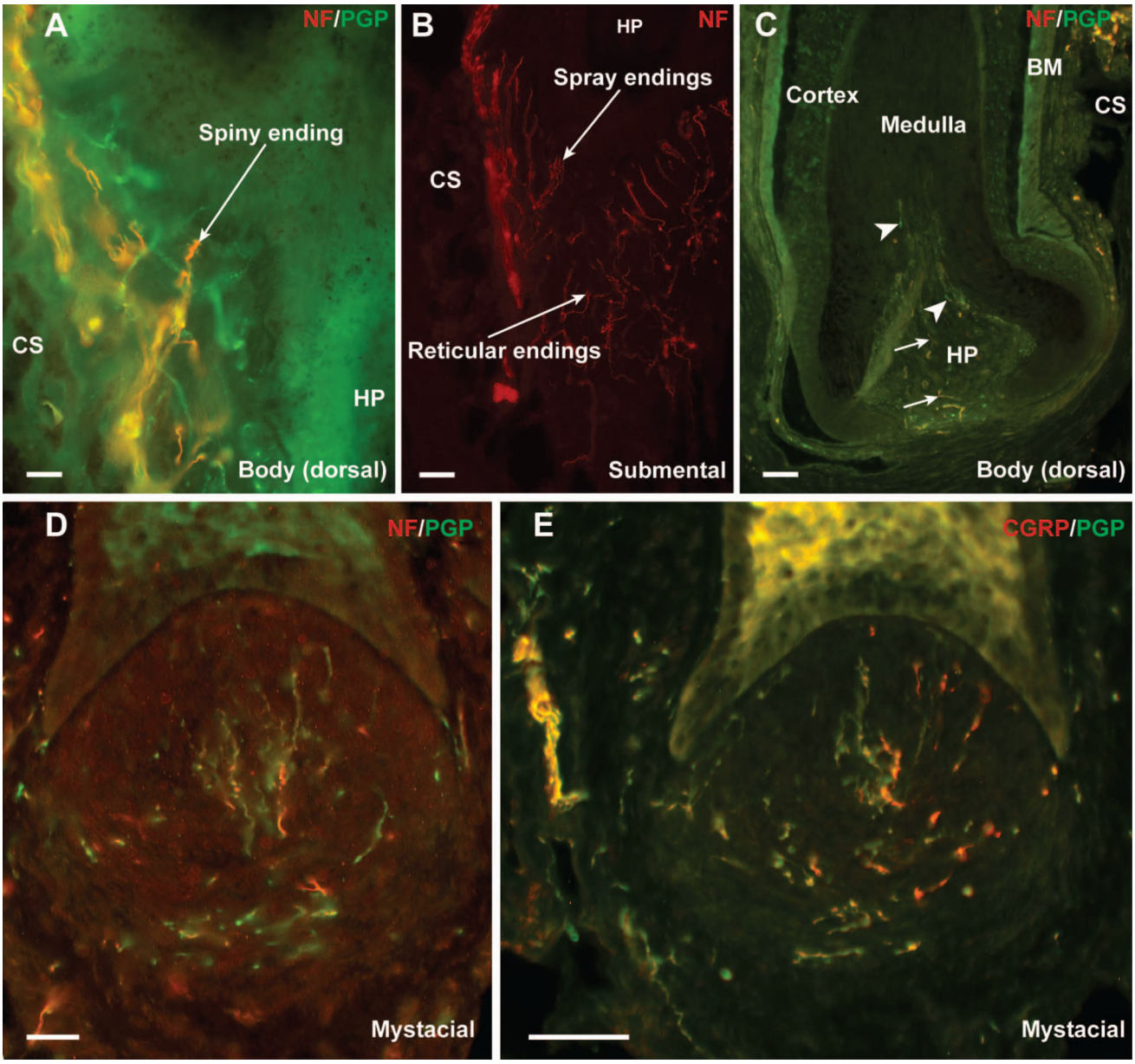


**Figure 8.**

Characterization of hyrax follicle-sinus complex (FSC) innervation at the cavernous sinus (CS) level, including innervation within the hair papilla (HP) (longitudinal planes of section). A) Spiny ending at the superficial CS level of a dorsal body FSC. B) Submental FSC at the CS level showing spray and reticular endings immunolabeled for NF200. C-E) Limited C- and Aδ-fiber innervation (arrowheads pointing to NF200− labeling and arrows pointing to NF200+ labeling, respectively, in C) within the hair papilla was not superficially extensive (i.e., did not extend very far in the direction of the epidermis). Scale bars=300μm (A), 75μm (B, D), 150μm (C, E). BM = basement membrane.

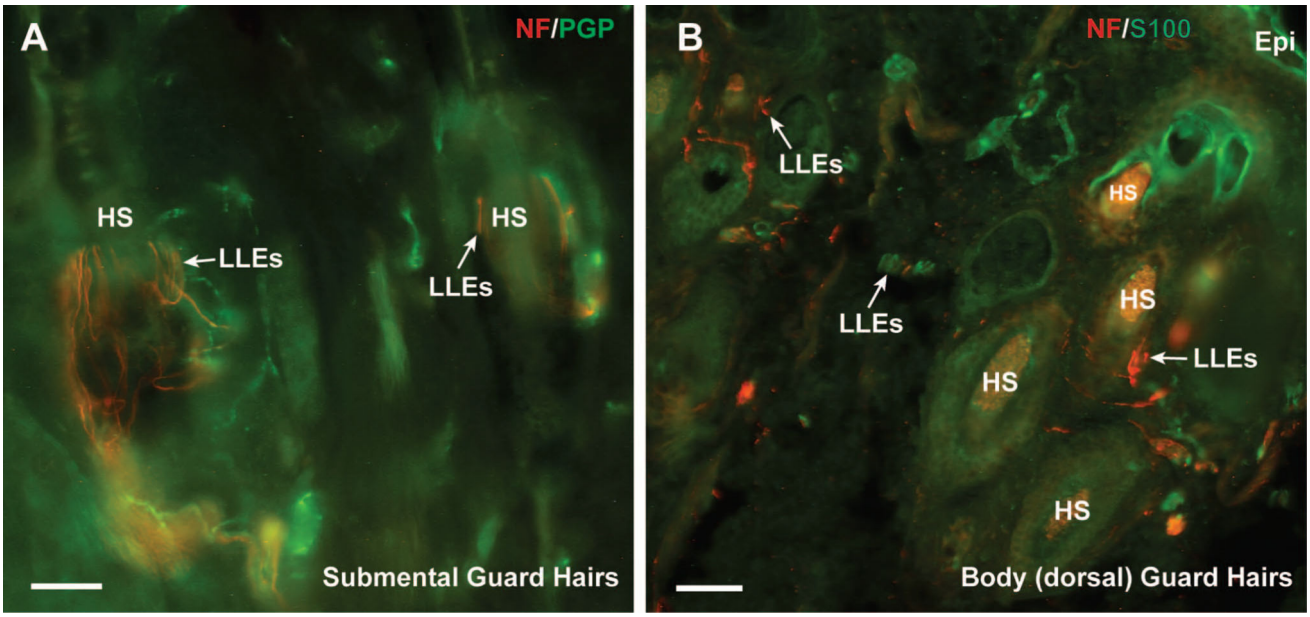


**Figure 9.**

Hyrax guard hair innervation. In contrast to FSCs, guard hairs lacked a circumferential ring sinus and exhibited only limited density and types of innervation. This innervation was characterized by piloneural complexes that included circumferential longitudinal lanceolate endings (A-B; longitudinal plane of section shown in A, oblique plane of section shown in B). Immunolabeling shown consisted of NF200 (red; 200kD subunit of neurofilament) paired with PGP (green, universal neuronal marker; protein gene product 9.5) or S100 (green, glial and ependymal marker). Scale bars=150μm. Epi = epidermis, HS = hair shaft, LLEs = longitudinal lanceolate endings.